

Givens QR Decomposition over Relational Databases

Dan Olteanu
olteanu@ifi.uzh.ch
University of Zurich
Zurich, Switzerland

Nils Vortmeier
nils.vortmeier@uzh.ch
University of Zurich
Zurich, Switzerland

Dorđe Živanović
dorđe.zivanovic@cs.ox.ac.uk
University of Oxford
Oxford, United Kingdom

ABSTRACT

This paper introduces FiGARo, an algorithm for computing the upper-triangular matrix in the QR decomposition of the matrix defined by the natural join over a relational database. The QR decomposition lies at the core of many linear algebra techniques and their machine learning applications, including: the matrix inverse; the least squares; the singular value decomposition; eigenvalue problems; and the principal component analysis.

FiGARo’s main novelty is that it pushes the QR decomposition past the join. This leads to several desirable properties. For acyclic joins, it takes time linear in the database size and independent of the join size. Its execution is equivalent to the application of a sequence of Givens rotations proportional to the join size. Its number of rounding errors relative to the classical QR decomposition algorithms is on par with the input size relative to the join size.

In experiments with real-world and synthetic databases, FiGARo outperforms both in runtime performance and accuracy the LAPACK libraries openblas and Intel MKL by a factor proportional to the gap between the join output and input sizes.

CCS CONCEPTS

• Information systems → Data management systems; • Mathematics of computing → Computations on matrices.

KEYWORDS

QR decomposition, Givens rotations, database joins

1 INTRODUCTION

This paper revisits the fundamental problem of computing the QR decomposition: Given a matrix $A \in \mathbb{R}^{m \times n}$, its (thin) QR decomposition is the product of the orthogonal matrix $Q \in \mathbb{R}^{m \times n}$ and the upper-triangular matrix $R \in \mathbb{R}^{n \times n}$ [23]. It originated seven decades ago in works by Rutishauser [34] and Francis [16]. There are three classical algorithms for QR decomposition: Gram-Schmidt and its modified version [22, 38], Householder [24], and Givens rotations [19]. This decomposition lies at the core of many linear algebra techniques and their machine learning applications [21, 39, 41] such as the matrix (pseudo) inverse and the least squares used in the closed-form solution for linear regression. In particular, the upper-triangular matrix R shares the same singular values with A ; its singular value decomposition can be used for the principal component analysis of A ; it constitutes a Cholesky decomposition of $A^T A$, which is used for training (non)linear regression models using gradient descent [37]; the product of its diagonal entries equals (ignoring the sign) the determinant of A , the product of the eigenvalues of A , and the product of the singular values of A .

In the classical linear algebra setting, the input matrix A is fully materialized and the process that constructs A is irrelevant. Our

database setting is different: A is not materialized and instead defined symbolically by the join of the relations in the input database. Our goal is to compute the decomposition of A without explicitly constructing A . This is desirable in case A is larger than the input database. By pushing the decomposition past the join down to the input relations, the runtime improvement is proportional to the size gap between the materialized join output and the input database.

This database setting has been used before for learning over relational data [31]. Joins are used to construct the training dataset from all available data sources and are unselective by design (the more labelled samples available for training, the better). This is not only the case for many-to-many joins; even key-fkey joins may lead to large (number of values in the) output, where data functionally determined by a key in a relation is duplicated in the join output as many times as this key appears in the join output. By avoiding the materialization of this large data matrix and pushing the learning task past the joins, learning can be much faster than over the materialized matrix [31]. Prior instances of this setting include pushing sum aggregates past joins [27, 43] and eager confidence computation in probabilistic databases [32].

This paper introduces FiGARo, an algorithm for computing the upper-triangular matrix R in the QR decomposition of the matrix A defined by the natural join of the relations in the input database. The acronym FiGARo stands for **F**actorized **G**ivens **R**otations with **a** and **i** swapped. FiGARo enjoys several desirable properties.

- For acyclic joins it takes time linear in the input data size and independently of the (potentially much larger) join output. It achieves this by pushing the computation past the joins.
- Its execution is equivalent to a sequence of Givens rotations over the join output. Yet instead of effecting the rotations individually as in the classical Givens QR decomposition, it performs fast block transformations whose effects are the same as for long sequences of rotations.
- It can be more accurate than the QR decomposition algorithm in mainstream linear algebra packages such as MKL and openblas, as it introduces far less rounding errors than the latter in case the join output is larger than the input database.
- Its transformations can be applied independently, so in parallel, to disjoint blocks of rows and also to different columns.

Once R is computed, the orthogonal matrix Q can be computed efficiently as AR^{-1} , again without materializing A [10].

Our work complements prior work on linear algebra computation powered by database engines [7, 14, 29, 35, 45] and on languages that unify linear algebra and relational algebra [13, 17, 25]. No prior work considered the interaction of QR decomposition with database joins. This requires a redesign of the decomposition algorithm from first principles. FiGARo is the first approach to take advantage of the structure and sparsity of relational data to improve the performance and accuracy of QR decomposition.

We introduce FiGARo in several steps. We first explain how it works on the materialized join (Section 4) and then on the unmaterIALIZED join modelled on any of its join trees (Section 6). FiGARo requires the computation of a batch of group-by counts over the join. This can be done in only two passes over the input database (Section 5). To obtain the desired upper-triangular matrix, FiGARo's output is further post-processed (Section 7).

FiGARo can outperform both in runtime performance and accuracy the LAPACK libraries openblas and Intel MKL by a factor proportional to the gap between the join output and input sizes, which is up to three orders of magnitude in our experiments (Section 8). We show this to be the case for both key - foreign key joins over two real-world databases and for many-to-many joins of one real-world and one synthetic database. We considered matrices with 2M-125M rows (84M-150M rows in the join matrix) and both narrow (up to 50 data columns) and wide (up to thousands of data columns). We show that the choice of the join tree and also the lack thereof can significantly influence the performance (up to 394x).

We designed an accuracy experiment for QR decomposition that may be of independent interest. Commonly, one checks the accuracy of one system relative to another or how close the computed Q is to an orthogonal matrix. Instead, we introduce a reverse engineering approach that defines a database of two relations from a fragment of an upper-triangular matrix R , whose values can be chosen arbitrarily and serve as ground truth. Then, R is obtained by the QR decomposition of the Cartesian product of these relations.

1.1 Givens Rotations on the Cartesian Product

We next show how FiGARo works on a simple example. Consider

the matrices $S = \begin{bmatrix} s_1 \\ \dots \\ s_p \end{bmatrix}$, $T = \begin{bmatrix} t_1 \\ \dots \\ t_q \end{bmatrix}$, and $A = \begin{bmatrix} A_1 \\ \dots \\ A_p \end{bmatrix}$, where A_i is

the $q \times 2$ matrix block $\begin{bmatrix} s_i & t_1 \\ \dots & \dots \\ s_i & t_q \end{bmatrix}$ for $i \in [p]$. The matrices S and T

represent unary relations $S(Y_1)$ and $T(Y_2)$, where the row order and attribute names make up the *contextual information* needed to map between relations and matrices [13]. The order of the rows does not matter for our computation: Consider any permutation P of the rows in A . Then, $PA = (PQ)R$ so the permutation only affects the orthogonal matrix Q and not the upper-triangular matrix R . We thus only need to keep the attribute names as contextual information as we move from relations to matrices. The $pq \times 2$ matrix A represents the Cartesian product of these two unary relations. We would like to compute the QR decomposition of A : $A = QR$.

The classical Givens rotations algorithm needs time quadratic in the input S and T : it constructs the upper-triangular matrix R from A using $2pq - 3$ rotations, one rotation for zeroing each cell below the diagonal in A . This takes $13(2pq - 3)$ multiplication, division, square, and square root operations. In contrast, FiGARo constructs R from S and T in linear time using $30(p + q)$ such operations.

We next explain key ideas behind this speed-up improvement. In later sections we apply them to equality joins, which are unions of Cartesian products, and then to join trees, which are evaluation orders for conjunctions of joins.

A 2×2 Givens rotation matrix is a matrix $G = \begin{bmatrix} c & -s \\ s & c \end{bmatrix}$ with $c = \cos \theta$ and $s = \sin \theta$ for some angle θ . If θ is selected appropriately, applying a Givens rotation introduces zeros in matrices. Consider a matrix $B = \begin{bmatrix} a \\ b \end{bmatrix}$, where a, b are real numbers with $b \neq 0$. Let us choose θ such that $\sin \theta = -\frac{\text{sign}(a)b}{\sqrt{a^2+b^2}}$ and $\cos \theta = \frac{|a|}{\sqrt{a^2+b^2}}$ [4]. The application of the rotation G to the matrix B is effected by the multiplication of the two matrices: $GB = \begin{bmatrix} r \\ 0 \end{bmatrix}$, where $r = \text{sign}(a)\sqrt{a^2+b^2}$. A sequence of Givens rotations can be used to set all entries below the diagonal of any matrix A to 0, thus obtaining an upper triangular matrix. The left multiplication of these rotation matrices yields the orthogonal matrix Q in the QR decomposition of A .

Let us apply Givens rotations to each block A_i independently and first set all but the first occurrence of s_i to 0. Using the rotation with $\sin \theta = -\frac{\text{sign}(s_i)s_i}{\sqrt{s_i^2+s_i^2}} = -\frac{1}{\sqrt{2}}$ and $\cos \theta = \frac{|s_i|}{\sqrt{s_i^2+s_i^2}} = \frac{1}{\sqrt{2}}$, the first occurrence of s_i is replaced by $\text{sign}(s_i)\sqrt{s_i^2+s_i^2} = \sqrt{2}s_i$ and the second occurrence becomes 0. For the second rotation, we choose θ based on the value $\sqrt{2}s_i$ of the first entry and the value s_i of the third entry of the first column, with the aim of setting the latter to 0. This is achieved with $\sin \theta = -\frac{1}{\sqrt{3}}$ and $\cos \theta = \frac{\sqrt{2}}{\sqrt{3}}$. This rotation sets the first entry to $\sqrt{3}s_i$. This argument can be continued: the rotation, which is used to set the k -th occurrence of s_i to 0, has $\sin \theta = -\frac{1}{\sqrt{k}}$ and $\cos \theta = \frac{\sqrt{k-1}}{\sqrt{k}}$.

INSIGHT 1. For the matrix A_i , there is a sequence G_s of Givens rotations that sets the first occurrence of s_i to $s_i\sqrt{q}$ and all other occurrences to 0. G_s is independent of the values in A_i .

We can use G_s for all blocks A_i to set all occurrences of s_i but the first one to 0. This yields the blocks $A'_i = \begin{bmatrix} s_i\sqrt{q} & t'_1 \\ 0 & t'_2 \\ \dots & \dots \\ 0 & t'_q \end{bmatrix}$, where the values t'_j can be computed from T in time $O(q)$, cf. Section 3.

INSIGHT 2. G_s yields the same values t'_1, \dots, t'_q in each matrix A'_i . These values can be computed once.

Rotations similar to G_s can now be applied to each block of p equal rows $[0 \ t'_j]$ for $2 \leq j \leq q$, to yield one row $[0 \ t'_j\sqrt{p}]$ and $p-1$ rows $[0 \ 0]$. We can further rotate the p rows $[s_i\sqrt{q} \ t'_1]$ for $1 \leq i \leq p$, to yield one row $[s'_i\sqrt{q} \ t'_1\sqrt{p}]$ and $p-1$ rows $[s'_i\sqrt{q} \ 0]$, for $2 \leq i \leq p$, where the values s'_i can be computed from S in time $O(p)$ by the same recurrence formula mentioned above (Section 3).

Together, this yields the matrix A'' that consists of the blocks

$$A''_1 = \begin{bmatrix} s'_1\sqrt{q} & t'_1\sqrt{p} \\ 0 & t'_2\sqrt{p} \\ \dots & \dots \\ 0 & t'_q\sqrt{p} \end{bmatrix} \text{ and } A''_i = \begin{bmatrix} s'_i\sqrt{q} & 0 \\ 0 & 0 \\ \dots & \dots \\ 0 & 0 \end{bmatrix} \text{ for } 2 \leq i \leq p.$$

At this point, four key observations can be drawn:

- (1) The matrix A'' has only $p+q$ non-zero values. All zero rows need not be represented as they are not part of the result R .
- (2) The values in A'' can be computed in one pass over S and T . We need to compute: \sqrt{p} , \sqrt{q} , and the values $s'_1, \dots, s'_p, t'_1, \dots, t'_q$.

(3) The computation of the values in A'' does not require taking the squares of the input values, as done by the Givens QR decomposition. This means less rounding errors that would otherwise appear when squaring very large or very small input values.

(4) Our linear-time computation of the non-zero entries in A'' yields the same result as quadratically many Givens rotations.

A post-processing step further brings A'' into the sought upper-triangular matrix R by applying a sequence of $p + q - 3$ rotations to zero all but the top three non-zero values.

To sum up, FiGARo only needs $O(p + q)$ time to compute R in our example. Including post-processing, the number of necessary computations of squares, square roots, multiplications and divisions is at most $4(p + q)$, $3(p + q)$, $17(p + q)$ and $6(p + q)$, respectively. In contrast, the Givens QR decomposition working on the materialized Cartesian product takes $O(pq)$ time and computes $4pq$ squares, $2pq$ square roots, $16pq$ multiplications and $4pq$ divisions.

The linear-time behaviour of FiGARo holds for matrices defined by any acyclic join over arbitrary relations. In contrast, the runtime of any algorithm, which works on the materialized join output, as well as its square, square root, multiplication, and division computations are proportional to the size of the join output.

2 THE FIGARO ALGORITHM: SETUP

Relations and Joins. A database \mathcal{D} consists of a set S_1, \dots, S_r of relations. Each relation has a schema (Z_1, \dots, Z_k) , which is a tuple of attribute names, and contains a set of tuples over this schema. We denote tuples (Z_1, \dots, Z_ℓ) of attribute names by \bar{Z} and tuples (z_1, \dots, z_ℓ) of values by \bar{z} . For every relation S_i , we denote by \bar{X}_i the tuple of its *key* (join) attributes and by \bar{Y}_i the tuple of the *data* (non-join) attributes. We allow key values of any type, e.g., categorical, while the data values are real numbers. We denote by \bar{X}_{ij} the join attributes common to both relations S_i and S_j . We consider the natural join of all relations in a database and write \bar{X} and \bar{Y} for the tuple of all key and data attributes in the join output. A database is *fully reduced* if there is no dangling input tuple that does not contribute to the join output. A join is (α)-acyclic if and only if it admits a *join tree* [1]: In a join tree, each relation is a node and for two relations S_i and S_j , all nodes on the unique path between the nodes for S_i and S_j correspond to relations whose keys include \bar{X}_{ij} .

From Relations to Matrices. Let $[n] = \{1, \dots, n\}$ for a natural number n . Matrices are denoted by bold upper-case letters, (column) vectors by bold lower-case letters. Consider a matrix A with m rows and n columns, a row index $i \in [m]$ and a column index $j \in [n]$. Then $A[i : j]$ is the entry in row i and column j , $A[i :]$ is the i -th row, $A[:, j]$ is the j -th column of A , and $|A|$ is the number of rows in A . For sets $I \subseteq [m]$ and $J \subseteq [n]$, $A[I : J]$ is the matrix consisting of the rows and columns of A indexed by I and J , respectively.

Each relation S_i is encoded by a matrix S_i that consists of all rows $(\bar{x}_i, \bar{y}_i) \in S_i$. The relation representing the output of the natural join of the input relations is encoded by the matrix A whose rows (\bar{x}, \bar{y}) are over the key attributes \bar{X} and data attributes \bar{Y} . We keep the keys and the column names as *contextual information* [13] to facilitate convenient reference to the data in the matrix. For ease of presentation, in this paper we use relations and matrices interchangeably following our above mapping. We use relational algebra over matrices to mean over the relations they encode.

We use an indexing scheme for matrices that exploits their relational nature. We refer to the matrix columns by their corresponding attribute names. We refer to the matrix rows and blocks by tuples of key and data values. Consider for example a ternary relation S with attribute names X, Y_1, Y_2 . We represent this relation as a matrix S such that for every tuple $(x, y_1, y_2) \in S$ there is a matrix row $S[x, y_1, y_2 :] = [x \ y_1 \ y_2]$ with entries $S[x, y_1, y_2 : X] = x$, $S[x, y_1, y_2 : Y_1] = y_1$, and $S[x, y_1, y_2 : Y_2] = y_2$. We will also use row indices that are different from the content of the row. We use $*$ to denote sets of indices. For example, $S[x, * : X, Y_1]$ denotes the block that contains all rows of S whose identifier starts with x , restricted to the columns X and Y_1 .

Input. The input to FiGARo consists of (1) the set of matrices S_1, \dots, S_r , one per relation in the input fully-reduced database \mathcal{D} , and (2) a join tree τ of the acyclic natural join of these matrices (or equivalently of the underlying relations). Arbitrary joins (including cyclic ones) can be supported by partial evaluation to acyclic joins: We construct a tree decomposition of the join and materialise its bags (sub-queries), cf. prior works on learning over joins, e.g., [33, 36, 37]. This partial evaluation incurs non-linear time. This is unavoidable under widely held conjectures.

Output. FiGARo computes the upper-triangular matrix R in the QR decomposition of the matrix block $A[:, \bar{Y}]$, which consists of the data columns \bar{Y} in the join of the database relations. It first computes an almost upper-triangular matrix R_0 such that $A[:, \bar{Y}] = Q_0 R_0$ for an orthogonal matrix Q_0 . A post-processing step (Section 7) further decomposes R_0 : $R_0 = Q_1 R$, where Q_1 is orthogonal. Thus, $A[:, \bar{Y}] = (Q_0 Q_1) R$, where the final orthogonal matrix is $Q = Q_0 Q_1$. FiGARo does not compute Q explicitly, it only computes R .

The QR decomposition always exists; whenever A has full rank, i.e., no column of A is a linear combination of other columns in A , and R has positive diagonal values, the decomposition is unique [41, Chapter 4, Theorem 1.1].

3 HEADS AND TAILS

Given a matrix, the classical Givens QR decomposition algorithm repeatedly zeroes the values below its diagonal. Each zero is obtained by one Givens rotation. In case the matrix encodes a join output, a pattern emerges: The matrix consists of blocks representing the Cartesian products of arbitrary matrices and one-row matrices (see Figure 1(a)). The effects of applying Givens rotations to such blocks are captured using so-called *heads* and *tails*. Before we introduce these notions, we recall the notion of Givens rotations.

Definition 3.1 (Givens rotation). A d -dimensional Givens rotation matrix is obtained from the d -dimensional identity matrix by changing four entries: $G[i : i] = G[j : j] = \cos \theta$, $G[i : j] = -\sin \theta$

and $G[j : i] = \sin \theta$, for some pair i, j of indices and an angle θ .

$$G = \begin{matrix} & & i & & j & & \\ \begin{matrix} 1 \\ \vdots \\ i \\ \vdots \\ j \\ \vdots \\ 0 \end{matrix} & \begin{matrix} \cdots & 0 & \cdots & 0 & \cdots & 0 \end{matrix} & \\ \begin{matrix} \vdots \\ \vdots \\ \vdots \\ \vdots \\ \vdots \\ \vdots \\ \vdots \end{matrix} & \begin{matrix} \ddots & \vdots & \ddots & \vdots & \ddots & \vdots \end{matrix} & \\ \begin{matrix} 0 \\ \vdots \\ 0 \\ \vdots \\ 0 \\ \vdots \\ 0 \end{matrix} & \begin{matrix} \cdots & \cos \theta & \cdots & -\sin \theta & \cdots & 0 \end{matrix} & \\ \begin{matrix} \vdots \\ \vdots \\ \vdots \\ \vdots \\ \vdots \\ \vdots \\ \vdots \end{matrix} & \begin{matrix} \vdots & \vdots & \ddots & \vdots & \ddots & \vdots \end{matrix} & \\ \begin{matrix} 0 \\ \vdots \\ 0 \\ \vdots \\ 0 \\ \vdots \\ 0 \end{matrix} & \begin{matrix} \cdots & \sin \theta & \cdots & \cos \theta & \cdots & 0 \end{matrix} & \\ \begin{matrix} \vdots \\ \vdots \\ \vdots \\ \vdots \\ \vdots \\ \vdots \\ \vdots \end{matrix} & \begin{matrix} \vdots & \vdots & \ddots & \vdots & \ddots & \vdots \end{matrix} & \\ 0 & \cdots & 0 & \cdots & 0 & \cdots & 1 \end{matrix}$$

We denote such a d -dimensional rotation matrix for given i, j and θ by $\text{Giv}_d(i, j, \sin \theta, \cos \theta)$. \square

A rotation matrix is orthogonal. The result $B = GA$ of the product of a rotation G and a matrix $A \in \mathbb{R}^{d \times d}$ is A except for the i -th and the j -th rows, which are subject to the counterclockwise rotation through the angle θ about the origin of the 2-dimensional Cartesian coordinate system: for each column c , $B[i : c] = A[i : c] \cos \theta - A[j : c] \sin \theta$ and $B[j : c] = A[i : c] \sin \theta + A[j : c] \cos \theta$.

The following notions are used throughout the paper. Given matrices $S \in \mathbb{R}^{m_1 \times n_1}$ and $T \in \mathbb{R}^{m_2 \times n_2}$, their Cartesian product $S \times T$

is the matrix $\begin{bmatrix} A_1 \\ \vdots \\ A_{m_1} \end{bmatrix} \in \mathbb{R}^{m_1 m_2 \times (n_1 + n_2)}$ with $A_i = \begin{bmatrix} S[i :] & T[1 :] \\ \vdots & \vdots \\ S[i :] & T[m_2 :] \end{bmatrix}$.

For $S \in \mathbb{R}^{1 \times n}$ and $v \in \mathbb{R}^m$, the Kronecker product $S \otimes v$ is $\begin{bmatrix} v[1]S \\ \vdots \\ v[m]S \end{bmatrix}$.

We denote by $\|v\|_2$ the ℓ_2 norm $\sqrt{\sum_{i=1}^m v[i]^2}$ of a vector $v \in \mathbb{R}^m$.

We now define the head and tail of a matrix, which we later use to express the Givens rotations over Cartesian products of matrices.

Definition 3.2 (Head and Tail). Let A be a matrix from $\mathbb{R}^{m \times n}$.

The *head* $\mathcal{H}(A) \in \mathbb{R}^{1 \times n}$ of A is the one-row matrix

$$\mathcal{H}(A) = \frac{1}{\sqrt{m}} \sum_{i=1}^m A[i :].$$

The *tail* $\mathcal{T}(A) \in \mathbb{R}^{(m-1) \times n}$ of A is the matrix (for $j \in [m-1]$)

$$\mathcal{T}(A)[j :] = \frac{1}{\sqrt{j+1}} \left(\sqrt{j} A[j+1 :] - \frac{\sum_{i=1}^j A[i :]}{\sqrt{j}} \right) \quad \square$$

Consider a matrix A representing the Cartesian product of a one-row matrix S and an arbitrary matrix T . Then A is obtained by extending each row in T with the one-row S , as in Figure 1(a). As exemplified in Section 1.1, if all but the first occurrence of S in A is to be replaced by zeros using Givens rotations, the specific sequence of rotations only depends on the number of rows of T and not on the entries of S . The result of these rotations can be described by the head and tail of T .

LEMMA 3.3. For any matrices $S \in \mathbb{R}^{1 \times n_1}$ and $T \in \mathbb{R}^{m \times n_2}$, let $A = S \times T \in \mathbb{R}^{m \times (n_1 + n_2)}$ be their Cartesian product. Let the Givens rotation matrix $R_i = \text{Giv}_m(1, i, -\frac{1}{\sqrt{i}}, \frac{\sqrt{i-1}}{\sqrt{i}})$, for all $i \in \{2, \dots, m\}$.

$$A = \begin{bmatrix} S & T \\ \vdots & \vdots \\ S & T \end{bmatrix} \rightsquigarrow \begin{matrix} \mathcal{H}(A) = \sqrt{m}S & \mathcal{H}(T) \\ \mathcal{T}(A) = \begin{bmatrix} 0 \\ \vdots \\ 0 \end{bmatrix} & \mathcal{T}(T) \end{matrix}$$

(a) Transformation of the Cartesian product of a one-row matrix S and an m -row matrix T .

$$A = \begin{bmatrix} v_1 S & T \\ \vdots & \vdots \\ v_m S & T \end{bmatrix} \rightsquigarrow \begin{matrix} \mathcal{H}(A, v) = \|v\|_2 S & \mathcal{H}(T, v) \\ \mathcal{T}(A, v) = \begin{bmatrix} 0 \\ \vdots \\ 0 \end{bmatrix} & \mathcal{T}(T, v) \end{matrix}$$

(b) Generalization of the transformation at (a), where S is scaled by a vector $v = (v_1, \dots, v_m)$ of positive real numbers.

Figure 1: Visualization of Lemmas 3.3 and 3.5: Matrices and results of applying the (generalized) head and tail.

Let $G = R_m \cdots R_2$ be the orthogonal matrix that is the product of the rotations R_m to R_2 .

The matrix $U = GA$ obtained by applying the rotations R_i to A is:

$$U = \begin{bmatrix} \mathcal{H}(A) \\ \mathcal{T}(A) \end{bmatrix} = \begin{bmatrix} \sqrt{m}S & \mathcal{H}(T) \\ 0^{(m-1) \times n_1} & \mathcal{T}(T) \end{bmatrix}.$$

In other words, the application of the $m-1$ rotations to A yields a matrix with four blocks: the head and tail of T , S scaled by the square root of the number m of rows in T , and zeroes over $m-1$ rows and n_1 columns. So instead of applying the rotations, we may compute these blocks directly from S and T .

We also encounter cases where blocks of matrices do not have the simple form depicted in Figure 1(a), but where the multiple copies of the one-row matrix S are scaled by different real numbers v_1 to v_m , as in Figure 1(b). In these cases, we cannot compute heads and tails as in Lemma 3.3 to capture the effect of a sequence of Givens rotations. However, a generalized version of heads and tails can describe these effects, as defined next.

Definition 3.4 (Generalized Head and Tail). For any vector $v \in \mathbb{R}_{>0}^m$ and matrix $A \in \mathbb{R}^{m \times n}$, the *generalized head* $\mathcal{H}(A, v) \in \mathbb{R}^{1 \times n}$ and *generalized tail* $\mathcal{T}(A, v) \in \mathbb{R}^{(m-1) \times n}$ of A weighted by v are:

$$\mathcal{H}(A, v) = \frac{1}{\|v\|_2} \sum_{i=1}^m v[i] A[i :]$$

$$\mathcal{T}(A, v)[j :] = \frac{1}{\|v[1, \dots, j+1]\|_2} \left(\|v[1, \dots, j]\|_2 A[j+1 :] - \frac{v[j+1] \sum_{i=1}^j v[i] A[i :]}{\|v[1, \dots, j]\|_2} \right) \quad \square$$

If v is the vector of ones, then $\|v\|_2 = \sqrt{m}$ and the generalized head and generalized tail become the head and tail, respectively.

We next generalize Lemma 3.3, where we consider each copy of S in A weighted by a positive scalar value from a weight vector v : the i -th row of T is appended by $v_i S$, for some positive real v_i , see Figure 1(b). This scaling is expressed using the Kronecker product \otimes . Here again, if we want to set all but the first (scaled) occurrences of

S to zero using Givens rotations, these rotations are independent of S and only depend on the scaling factors \mathbf{v} and the number of rows in T. We use $\mathcal{H}(\mathbf{A}, \mathbf{v})$ and $\mathcal{T}(\mathbf{A}, \mathbf{v})$ to construct the result of applying the rotations to A.

LEMMA 3.5. Let $\mathbf{v} \in \mathbb{R}_{>0}^m$, $\mathbf{S} \in \mathbb{R}^{1 \times n_1}$, and $\mathbf{T} \in \mathbb{R}^{m \times n_2}$ be given. Let $\mathbf{A} = [\mathbf{S} \otimes \mathbf{v} \quad \mathbf{T}] \in \mathbb{R}^{m \times (n_1 + n_2)}$. Let \mathbf{R}_i be the Givens rotation $\mathbf{R}_i = \text{Giv}_m(1, i, -\frac{\mathbf{v}[i]}{\|\mathbf{v}[1, \dots, i]\|_2}, \frac{\|\mathbf{v}[1, \dots, i-1]\|_2}{\|\mathbf{v}[1, \dots, i]\|_2})$, for all $i \in \{2, \dots, m\}$, and let G be the orthogonal matrix $\mathbf{G} = \mathbf{R}_m \cdots \mathbf{R}_2$. The matrix $\mathbf{U} = \mathbf{GA}$ obtained by applying the rotations \mathbf{R}_i to A is:

$$\mathbf{U} = \begin{bmatrix} \mathcal{H}(\mathbf{A}, \mathbf{v}) \\ \mathcal{T}(\mathbf{A}, \mathbf{v}) \end{bmatrix} = \begin{bmatrix} \|\mathbf{v}\|_2 \mathbf{S} & \mathcal{H}(\mathbf{T}, \mathbf{v}) \\ \mathbf{0}_{(m-1) \times n_1} & \mathcal{T}(\mathbf{T}, \mathbf{v}) \end{bmatrix}.$$

The generalized head and tail can be computed in linear time in the size of the input matrix A. We explain this for the tail. Given the ℓ_2 -norm of the vector \mathbf{v} restricted to the first j entries, we can compute the same norm of \mathbf{v} now restricted to the first $j+1$ entries in constant time. Likewise, the sum of the rows $\mathbf{v}[i] \mathbf{A}[i:]$ where i goes up to j can be reused to compute the sum of these rows up to $j+1$ in time proportional to the row length n .

LEMMA 3.6. Given any matrix $\mathbf{A} \in \mathbb{R}^{m \times n}$ and vector $\mathbf{v} \in \mathbb{R}_{>0}^m$, the generalized head $\mathcal{H}(\mathbf{A}, \mathbf{v})$ and the generalized tail $\mathcal{T}(\mathbf{A}, \mathbf{v})$ can be computed in time $O(mn)$.

The following lemma follows immediately from Definition 3.4.

LEMMA 3.7. For any matrix $\mathbf{A} \in \mathbb{R}^{m \times n}$, vector $\mathbf{v} \in \mathbb{R}_{>0}^m$, and numbers $k \in \mathbb{R}$ and $\ell \in \mathbb{R}_{>0}$, the following holds:

$$\begin{aligned} \mathcal{H}(k\mathbf{A}, \ell\mathbf{v}) &= k \mathcal{H}(\mathbf{A}, \mathbf{v}) \\ \mathcal{T}(k\mathbf{A}, \ell\mathbf{v}) &= k \mathcal{T}(\mathbf{A}, \mathbf{v}) \end{aligned}$$

4 EXAMPLE: ROTATIONS ON A JOIN OUTPUT

Section 1.1 shows how a Cartesian product of two matrices can be transformed into an almost upper-triangular matrix by applying Givens rotations. Section 3 subsequently shows how the same result can be computed in linear time from the input matrices using the new operations head and tail, whose effects on matrices of a special form are summarized in Lemmas 3.3 and 3.5.

Towards an algorithm for the general case, this section gives an example of applying Givens rotations to a matrix that represents the natural join of four input relations. The insights gained from this example lead to the formulation of the FiGARo algorithm.

Our approach is as follows. The result of joining two relations is a union of Cartesian products: for each join key \bar{x} , all rows from the first relation that have \bar{x} as their value for the join attributes are paired with all rows from the second relation with \bar{x} as their join value. We know from Section 1.1 and Section 3 how these Cartesian products can be processed. Then we take the union of their results, so, accumulate the resulting rows in a single matrix.

Figure 2 sketches the input matrices $\mathbf{S}_1, \dots, \mathbf{S}_4$ and the join tree τ used in this section. We explain \mathbf{S}_1 , the other matrices are similar. The matrix \mathbf{S}_1 in Figure 2(a) has a column X_{12} that represents the key attribute common with the matrix \mathbf{S}_2 . It contains two distinct values a_1 and a_2 for its join attribute X_{12} . For each a_j , there is one vector $\mathbf{S}_1^{a_j}$ of values for the data column Y_1 in \mathbf{S}_1 . The rows of \mathbf{S}_1 are the union of the Cartesian products $[a_j] \times \mathbf{S}_1^{a_j}$, for all $j \in \{1, 2\}$.

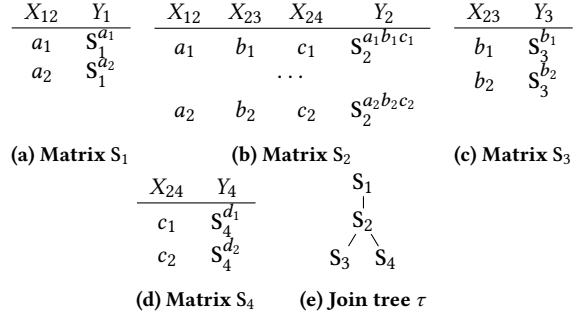


Figure 2: Matrices and join tree used in Section 4.

The output A of the natural join of $\mathbf{S}_1, \dots, \mathbf{S}_4$ contains the Cartesian product

$$[a_j \ b_k \ c_\ell] \times \mathbf{S}_1^{a_j} \times \mathbf{S}_2^{a_j b_k c_\ell} \times \mathbf{S}_3^{b_k} \times \mathbf{S}_4^{c_\ell}$$

for every tuple (a_j, b_k, c_ℓ) of join keys, with $j, k, \ell \in \{1, 2\}$. As mentioned in Section 2, we want to transform the matrix $\mathbf{A}[\bar{Y}]$, i.e., the projection of A to the data columns \bar{Y} , into a matrix \mathbf{R}_0 that is almost upper-triangular. In particular, the number of rows with non-zero entries in \mathbf{R}_0 needs to be linear in the size of the input matrices. We do this by repeatedly identifying parts of the matrix $\mathbf{A}[\bar{Y}]$ that have the form depicted in Figure 1 and by applying Lemmas 3.3 and 3.5 to these parts. Recall that each of these applications corresponds to the application of a sequence of Givens rotations.

The matrix $\mathbf{A}[\bar{Y}]$ contains the rows with the following Cartesian product associated with the join keys (a_1, b_1, c_1) :

$$\frac{Y_1}{\mathbf{S}_1^{a_1}} \times \frac{Y_2}{\mathbf{S}_2^{a_1 b_1 c_1}} \times \frac{Y_3}{\mathbf{S}_3^{b_1}} \times \frac{Y_4}{\mathbf{S}_4^{c_1}}$$

In turn, this Cartesian product is the union of Cartesian products $[t_1 \ t_2 \ t_3] \times \mathbf{S}_4^{c_1}$, for each choice t_1, t_2, t_3 of rows of $\mathbf{S}_1^{a_1}, \mathbf{S}_2^{a_1 b_1 c_1}$ and respectively $\mathbf{S}_3^{b_1}$. The latter products have the form depicted in Figure 1(a): the Cartesian product of a one-row matrix $[t_1 \ t_2 \ t_3]$ and an arbitrary matrix $\mathbf{S}_4^{c_1}$. By applying Lemma 3.3 to each of them, we obtain the following rows, where we use $\alpha = \sqrt{|\mathbf{S}_4^{c_1}|}$:

$$\begin{array}{cccc} Y_1 & Y_2 & Y_3 & Y_4 \\ \alpha \mathbf{S}_1^{a_1} & \times & \alpha \mathbf{S}_2^{a_1 b_1 c_1} & \times & \alpha \mathbf{S}_3^{b_1} & \times & \mathcal{H}(\mathbf{S}_4^{c_1}) \\ 0 & & 0 & & 0 & & \mathcal{T}(\mathbf{S}_4^{c_1}) \\ \vdots & & \vdots & & \vdots & & \vdots \\ 0 & & 0 & & 0 & & \mathcal{T}(\mathbf{S}_4^{c_1}) \end{array}$$

This matrix contains one copy of $\mathcal{T}(\mathbf{S}_4^{c_1})$ for every choice of t_1, t_2, t_3 . More copies of $\mathcal{T}(\mathbf{S}_4^{c_1})$ arise when we analogously apply Lemma 3.3 to the rows of $\mathbf{A}[\bar{Y}]$ associated with join keys (a_j, b_k, c_1) different from (a_1, b_1, c_1) . In total, the number of copies of $\mathcal{T}(\mathbf{S}_4^{c_1})$ we obtain is

$$\sum_{j,k \in \{1,2\}} |\mathbf{S}_1^{a_j}| \cdot |\mathbf{S}_2^{a_j b_k c_1}| \cdot |\mathbf{S}_3^{b_k}| = |\sigma_{X_{24}=c_1}(\mathbf{S}_1 \bowtie \mathbf{S}_2 \bowtie \mathbf{S}_3)|,$$

so, the size of the join of all matrices except \mathbf{S}_4 , where the attribute X_{24} is fixed to c_1 . We denote this number by $\Phi_4^\circ(c_1)$.

We apply more Givens rotations to the rows of the form $[0 \ 0 \ 0] \times \mathcal{T}(S_4^{c_1})$. These are again Cartesian products, namely the Cartesian products of the zero matrix of dimension $\Phi_4^\circ(c_1) \times 3$ and each row t of $\mathcal{T}(S_4^{c_1})$. We can apply again Lemma 3.3 to these Cartesian products and obtain the rows

$$\begin{array}{cccc} Y_1 & Y_2 & Y_3 & Y_4 \\ 0 & 0 & 0 & \sqrt{\Phi_4^\circ(c_1)} \mathcal{T}(S_4^{c_1}) \\ 0 & 0 & 0 & 0 \\ \vdots & \vdots & \vdots & \vdots \\ 0 & 0 & 0 & 0. \end{array}$$

Rows that only contain zeros can be discarded, the other rows become part of the (almost upper-triangular) result matrix \mathbf{R}_0 .

We now turn back to the remaining rows, which are of the form

$$\frac{Y_1}{\alpha S_1^{a_1}} \times \frac{Y_2}{\alpha S_2^{a_1 b_1 c_1}} \times \frac{Y_3}{\alpha S_3^{b_1}} \times \frac{Y_4}{\mathcal{H}(S_4^{c_1})}.$$

As in the first step, we identify these rows as unions of (column-permutations of) Cartesian products $[at_1 \ at_2 \ \mathcal{H}(S_4^{c_1})] \times \alpha S_3^{b_1}$, for each choice t_1, t_2 of rows of $S_1^{a_1}$ and $S_2^{a_1 b_1 c_1}$, respectively. The corresponding applications of Lemma 3.3 yield the rows

$$\begin{array}{cccc} Y_1 & Y_2 & Y_3 & Y_4 \\ \gamma S_1^{a_1} \times \gamma S_2^{a_1 b_1 c_1} \times \alpha \mathcal{H}(S_3^{b_1}) \times \beta \mathcal{H}(S_4^{c_1}) & & & \\ 0 & 0 & \alpha \mathcal{T}(S_3^{b_1}) & 0 \\ \vdots & \vdots & \vdots & \vdots \\ 0 & 0 & \alpha \mathcal{T}(S_3^{b_1}) & 0 \end{array}$$

where $\beta = \sqrt{|S_3^{b_1}|}$ and $\gamma = \alpha\beta$. Considering also the rows that we obtain for join keys (a_j, b_1, c_ℓ) different from (a_1, b_1, c_1) , the resulting matrix has $\sum_{j \in \{1,2\}} |S_1^{a_j}| \cdot |S_2^{a_j b_1 c_1}|$ copies of $\sqrt{|S_4^{c_1}|} \mathcal{T}(S_3^{b_1})$ as well as $\sum_{j \in \{1,2\}} |S_1^{a_j}| \cdot |S_2^{a_j b_1 c_2}|$ copies of $\sqrt{|S_4^{c_2}|} \mathcal{T}(S_3^{b_1})$.

We apply further Givens rotations to the rows that consist of zeros and the scaled copies of $\mathcal{T}(S_3^{b_1})$. For each row t of $\mathcal{T}(S_3^{b_1})$, we apply this time Lemma 3.5 to the matrix of all scaled copies of t and three columns of zeros. The result contains some all-zero rows and one row with entry t scaled by the ℓ_2 norm of the vector of the original scaling factors. This factor is the square root of

$$\begin{aligned} & \sum_{j \in \{1,2\}} |S_1^{a_j}| \cdot |S_2^{a_j b_1 c_1}| \cdot \sqrt{|S_4^{c_1}|^2} + \sum_{j \in \{1,2\}} |S_1^{a_j}| \cdot |S_2^{a_j b_1 c_2}| \cdot \sqrt{|S_4^{c_2}|^2} \\ &= \sum_{j, \ell \in \{1,2\}} |S_1^{a_j}| \cdot |S_2^{a_j b_1 c_\ell}| \cdot |S_4^{c_\ell}| \\ &= |\sigma_{X_{23}=b_1}(S_1 \bowtie S_2 \bowtie S_4)|, \end{aligned}$$

which, similarly as above, is the size of the join of all matrices except S_3 , where the attribute X_{23} is fixed to b_1 . We denote this number by $\Phi_3^\circ(b_1)$. In summary, the result of applying Lemma 3.5 contains, besides some all-zero rows, the rows

$$\begin{array}{cccc} Y_1 & Y_2 & Y_3 & Y_4 \\ 0 & 0 & \sqrt{\Phi_3^\circ(b_1)} \mathcal{T}(S_3^{b_1}) & 0. \end{array}$$

The remaining columns are processed analogously. Up to now, the transformations result in all-zero rows, rows that contain the scaled tail of a part of an input matrix with other columns being 0,

and one row for every join key (a_j, b_k, c_ℓ) , for $j, k, \ell \in \{1, 2\}$. For fixed $a_j = a_1$, these rows are as follows, where for $k, \ell \in \{1, 2\}$ we use $\alpha_{k\ell} = \sqrt{|S_1^{a_1}| \cdot |S_2^{a_1 b_k c_\ell}| \cdot |S_3^{b_k}| \cdot |S_4^{c_\ell}|}$.

$$\begin{array}{cccc} Y_1 & Y_2 & Y_3 & Y_4 \\ \frac{\alpha_{11}}{\sqrt{|S_1^{a_1}|}} \mathcal{H}(S_1^{a_1}) & \frac{\alpha_{11}}{\sqrt{|S_2^{a_1 b_1 c_1}|}} \mathcal{H}(S_2^{a_1 b_1 c_1}) & \frac{\alpha_{11}}{\sqrt{|S_3^{b_1}|}} \mathcal{H}(S_3^{b_1}) & \frac{\alpha_{11}}{\sqrt{|S_4^{c_1}|}} \mathcal{H}(S_4^{c_1}) \\ & & \vdots & \\ \frac{\alpha_{22}}{\sqrt{|S_1^{a_1}|}} \mathcal{H}(S_1^{a_1}) & \frac{\alpha_{22}}{\sqrt{|S_2^{a_1 b_2 c_2}|}} \mathcal{H}(S_2^{a_1 b_2 c_2}) & \frac{\alpha_{22}}{\sqrt{|S_3^{b_2}|}} \mathcal{H}(S_3^{b_2}) & \frac{\alpha_{22}}{\sqrt{|S_4^{c_2}|}} \mathcal{H}(S_4^{c_2}) \end{array}$$

We observe that the entries in the column Y_1 only differ by the scaling factors $\alpha_{k\ell}$. We can apply Lemma 3.5, with $S = [\mathcal{H}(S_1^{a_1})]$, \mathbf{T} consisting of the columns Y_2, Y_3, Y_4 of the matrix above, and $\mathbf{v} =$

$$\begin{bmatrix} \frac{\alpha_{11}}{\sqrt{|S_1^{a_1}|}} \\ \vdots \\ \frac{\alpha_{22}}{\sqrt{|S_1^{a_1}|}} \end{bmatrix} = \begin{bmatrix} \sqrt{|S_1^{a_1}| \cdot |S_2^{a_1 b_1 c_1}| \cdot |S_3^{b_1}| \cdot |S_4^{c_1}|} \\ \sqrt{|S_1^{a_1}|} \\ \vdots \\ \sqrt{|S_1^{a_1}| \cdot |S_2^{a_1 b_2 c_2}| \cdot |S_3^{b_2}| \cdot |S_4^{c_2}|} \end{bmatrix} = \begin{bmatrix} \sqrt{|S_2^{a_1 b_1 c_1}| \cdot |S_3^{b_1}| \cdot |S_4^{c_1}|} \\ \vdots \\ \sqrt{|S_2^{a_1 b_2 c_2}| \cdot |S_3^{b_2}| \cdot |S_4^{c_2}|} \end{bmatrix}.$$

The first row of the result is the generalized head of the above rows. For column Y_1 , this is $\|\mathbf{v}\|_2 \mathcal{H}(S_1^{a_1})$, where $\|\mathbf{v}\|_2$ is equal to

$\sqrt{\sum_{k, \ell \in \{1,2\}} |S_2^{a_1 b_k c_\ell}| \cdot |S_3^{b_k}| \cdot |S_4^{c_\ell}|} = \sqrt{|\sigma_{X_{12}=a_1} S_2 \bowtie S_3 \bowtie S_4|}$. The term under the square root is the size of the join of all matrices in the subtree of S_3 in τ , where X_{12} is fixed to a_1 . We denote this number by $\Phi_3^\downarrow(a_1)$. We skip the discussion for the other columns.

The remaining rows are formed by the generalized tail. In column Y_1 , these rows only have zeros. For column Y_4 , the result is

$$\sqrt{|S_1^{a_1}|} \mathbf{T}_{4,a_1}, \text{ where } \mathbf{T}_{4,a_1} = \mathcal{T} \left(\begin{bmatrix} \sqrt{|S_2^{a_1 b_1 c_1}| \cdot |S_3^{b_1}| \cdot |S_4^{c_1}|} \\ \vdots \\ \sqrt{|S_2^{a_1 b_2 c_2}| \cdot |S_3^{b_2}| \cdot |S_4^{c_2}|} \end{bmatrix}, \mathbf{v} \right), \text{ and}$$

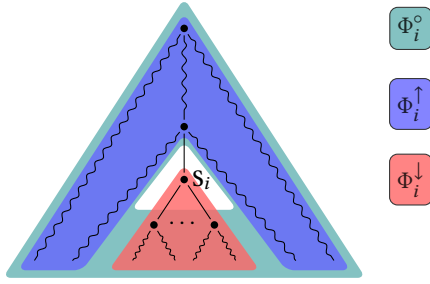
analogously for the columns Y_2 and Y_3 .

Remark 4.1. Suppose S_1 would have another child S_5 in τ , so, S_1 would also have the join attributes X_{15} . Then we would get one scaled copy of \mathbf{T}_{4,a_1} for every value of X_{15} that occurs together with the value a_1 for X_{12} . We would then apply Lemma 3.5 again. The scaling factor for \mathbf{T}_{4,a_1} we obtain in the general case is the square root of the size of the join of all relations that are *not* in the subtree of S_3 in τ , where X_{12} is fixed to a_1 . In the simple case considered here, this value is exactly $\sqrt{|S_1^{a_1}|}$.

To sum up, the resulting non-zero rows are of the form:

- (1) $\sqrt{\Phi_i^\circ(\bar{x}_i)} \mathcal{T}(S_i^{\bar{x}_i})$, for all $i \in [4]$ and values \bar{x}_i for the join attributes of S_i ,
- (2) $\sqrt{|S_1^{a_j}|} [\mathbf{T}_{2,a_j} \ \mathbf{T}_{3,a_j} \ \mathbf{T}_{4,a_j}]$, for $j \in \{1, 2\}$, and
- (3) one row of scaled generalized heads for each a_1 and a_2 .

The number of rows of type (1) is bounded by the overall number of rows in the input matrices minus the number of different join keys, as the tail of a matrix has one row less than the input matrix. The number of rows of type (2) is bounded by the different values for the join attributes (X_{12}, X_{23}, X_{24}) minus the number of different values for X_{12} . The number of rows of type (3) is bounded by the different values for the join attribute X_{12} . Together, the number of



$$\begin{aligned}\Phi_i^\circ(\bar{x}_i) &= \left| \sigma_{\bar{X}_i=\bar{x}_i} \left(\bigotimes_{j \in [r], j \neq i} S_j \right) \right| \\ \Phi_i^\uparrow(\bar{x}_p) &= \left| \sigma_{\bar{X}_p=\bar{x}_p} \left(\bigotimes_{\substack{j \in [r] \\ S_j \text{ is not in the subtree of } S_i}} S_j \right) \right| \\ \Phi_i^\downarrow(\bar{x}_p) &= \left| \sigma_{\bar{X}_p=\bar{x}_p} \left(\bigotimes_{\substack{j \in [r] \\ S_j \text{ is in the subtree of } S_i}} S_j \right) \right|\end{aligned}$$

Figure 3: Count queries used by FiGaRo, defined over the join tree τ of the r input matrices S_1, \dots, S_r . \bar{X}_i are the join attributes of S_i and \bar{X}_p are the join attributes that S_i has in common with its parent in τ . Φ_i° gives the number of tuples in the join of all relations except S_i , grouped by the attributes \bar{X}_i . Φ_i^\uparrow and Φ_i^\downarrow give the number of tuples in the join of the relations that are in the subtree of S_i in τ respectively not in this subtree, grouped by the attributes \bar{X}_p .

non-zero rows is bounded by the overall number of rows in the input matrices, as desired.

5 SCALING FACTORS AS COUNT QUERIES

The example in Section 1.1 applies Givens rotations to a Cartesian product. The resulting matrix uses scaling factors that are square roots of the numbers of rows of the input matrices. These numbers can be trivially computed directly from these matrices. In case of a matrix defined by joins, as seen in the preceding Section 4, these scaling factors are defined by group-by count queries over the joins. FiGaRo needs three types of such count queries at each node in the join tree. They can be computed together in linear time in the size of the input matrices. This section defines these queries and explains how to compute them efficiently.

We define the count queries Φ_i° , Φ_i^\uparrow and Φ_i^\downarrow for each input matrix S_i in a given join tree τ ($i \in [r]$). Figure 3 depicts graphically the meaning of these count queries: They give the sizes of joins of subsets of the input matrices, grouped by various join attributes of S_i : Φ_i^\uparrow and Φ_i^\downarrow join all matrices above and respectively below S_i in the join tree τ , while Φ_i° joins all matrices except S_i .

Each of these aggregates can be computed individually in time linear in the size of the input matrices using standard techniques for group-by aggregates over acyclic joins [33, 43]. This section shows how to further speed up their evaluation by identifying and executing common computation across all these aggregates. This

reduces the necessary number of scans of each of the input matrices from $\mathcal{O}(r)$ scans to two scans.

We recall our notation: τ be the join tree; \bar{X}_i are the join attributes of S_i and \bar{X}_{ij} are the common join attributes of S_i and its child S_j in τ . We assume that: each matrix S_j is sorted on the attributes \bar{X}_{ij} ; and a child S_j of S_i in τ is first sorted on the attributes \bar{X}_{ij} .

We first initialize the counts $\text{ROWS_PER_KEY}_i(\bar{x}_i)$ for each matrix S_i and value \bar{x}_i for its join attributes \bar{X}_i . These counts give the number of those rows in S_i that contain the join key \bar{x}_i for the columns \bar{X}_i . This step is done in one pass over the sorted matrices and takes linear time in their size. The aggregates Φ_i^\downarrow are computed in the same data pass. The computation of the aggregates Φ_i° and Φ_i^\uparrow is done in a second pass over the matrices. We utilize the following relationships between the aggregates.

Computing Φ_i^\downarrow : This aggregate gives the size of the join of the matrices in the subtree of S_i in τ grouped by the join attributes \bar{X}_p that are common to S_i and its parent in τ . If S_i is a leaf in τ , then $\bar{X}_p = \bar{X}_i$ and $\Phi_i^\downarrow(\bar{x}_i) = \text{ROWS_PER_KEY}_i(\bar{x}_i)$. If S_i is not a leaf in τ , then we compute the intermediate aggregate

$$\Theta_i^\downarrow(\bar{x}_i) = \left| \sigma_{\bar{X}_i=\bar{x}_i} \left(\bigotimes_{\substack{j \in [r] \\ S_j \text{ is in the subtree of } S_i}} S_j \right) \right|$$

which gives the size of the join of the same matrices as Φ_i^\downarrow , but grouped by \bar{X}_i instead of \bar{X}_p . The reason for computing Θ_i^\downarrow is that it is useful for other aggregates as well, as discussed later. This aggregate can also be expressed as

$$\Theta_i^\downarrow(\bar{x}_i) = \text{ROWS_PER_KEY}_i(\bar{x}_i) \cdot \prod_{\text{child } S_j \text{ of } S_i} \Phi_j^\downarrow(\bar{x}_{ij}),$$

where \bar{x}_{ij} is the projection of \bar{x}_i to the join attributes \bar{X}_{ij} . The aggregate $\Phi_i^\downarrow(\bar{x}_p)$ is then obtained by summing all values $\Theta_i^\downarrow(\bar{x}_i)$ such that \bar{x}_i projected to \bar{X}_p equals \bar{x}_p .

All aggregates $\Phi_1^\downarrow, \dots, \Phi_r^\downarrow$ can thus be computed in a bottom-up traversal of the join tree τ and in one pass over the sorted matrices.

Computing Φ_i^\uparrow : This aggregate is defined similarly to Φ_i^\downarrow , where the join is now over all matrices that are *not* in the subtree of S_i in the join tree τ . It is computed in a top-down traversal of τ .

Assume $\Phi_i^\uparrow(\bar{x}_p)$ is already computed, where \bar{x}_p is a value for the join attributes \bar{X}_p that S_i has in common with its parent in τ . We define the intermediate aggregate $\text{FULL_JOIN_SIZE}_i(\bar{x}_i) = \Phi_i^\uparrow(\bar{x}_p) \cdot \Theta_i^\downarrow(\bar{x}_i)$. It gives the size of the join over all matrices, grouped by \bar{X}_i . For the root S_1 of τ , we set $\text{FULL_JOIN_SIZE}_1(\bar{x}_1) = \Theta_1^\downarrow(\bar{x}_1)$.

We next define aggregates $\text{FULL_JOIN_SIZE}_{ij}(\bar{x}_{ij})$ that give the size of the join of all matrices for each value of the join attributes \bar{X}_{ij} that are common to S_i and its child S_j . They can be computed by summing up the values $\text{FULL_JOIN_SIZE}_i(\bar{x}_i)$ for the keys \bar{x}_i that agree with \bar{x}_{ij} on \bar{X}_{ij} . Since this size is the product of $\Phi_j^\downarrow(\bar{x}_{ij})$ and $\Phi_i^\uparrow(\bar{x}_{ij})$, we have $\Phi_i^\uparrow(\bar{x}_{ij}) = \text{FULL_JOIN_SIZE}_{ij}(\bar{x}_{ij}) / \Phi_j^\downarrow(\bar{x}_{ij})$, where Φ_j^\downarrow is already computed. For all children S_j of S_i , the sums $\text{FULL_JOIN_SIZE}_{ij}$ can be computed together in one pass over S_i .

Computing Φ_i° : This aggregate gives the size of the join of all matrices except S_i , grouped by the attributes \bar{X}_i . If S_i is a leaf in τ ,

Algorithm 1: Computing the count aggregates for FiGARo.

```

1 COMPUTE-COUNTS(matrices  $S_1, \dots, S_r$ , join tree  $\tau$ )
   $\triangleright \Phi_i^\downarrow, \Phi_i^\uparrow, \Phi_i^\circ, \text{ROWS\_PER\_KEY}_i$  and  $\Theta_i^\downarrow$  are initially empty ordered
    maps, for every matrix  $S_i$  (for the root  $S_r$  of  $\tau$ ,  $\Phi_r^\downarrow, \Phi_r^\uparrow$  do not exist).
2 PASS1(1)
3 PASS2(1)
4 PASS1 (index  $i$ )
   $\triangleright$  Computes  $\Phi_i^\downarrow$  and intermediate maps  $\text{ROWS\_PER\_KEY}_i, \Theta_i^\downarrow$ .
5 foreach child  $S_j$  of  $S_i$  in  $\tau$  do
6   PASS1( $j$ )
7   foreach value  $\bar{x}_i$  of the join attributes  $\bar{X}_i$  of  $S_i$  do
8      $\text{ROWS\_PER\_KEY}_i(\bar{x}_i) \leftarrow |\sigma_{\bar{X}_i=\bar{x}_i} S_i|$ 
9      $\Theta_i^\downarrow(\bar{x}_i) \leftarrow \text{ROWS\_PER\_KEY}_i(\bar{x}_i)$ 
10    foreach child  $S_j$  of  $S_i$  in  $\tau$  do
11       $\triangleright$  let  $\bar{x}_{ij}$  be the projection of  $\bar{x}_i$  onto  $\bar{X}_{ij}$ , the join attributes
        shared between  $S_i$  and  $S_j$ 
12       $\Theta_i^\downarrow(\bar{x}_i) \leftarrow \Theta_i^\downarrow(\bar{x}_i) \cdot \Phi_j^\downarrow(\bar{x}_{ij})$ 
13      if  $S_i$  is not the root of  $\tau$  then
14         $\triangleright$  let  $\bar{x}_p$  be the projection of  $\bar{x}_i$  onto the join attributes shared
          between  $S_i$  and its parent in  $\tau$ 
15         $\Phi_i^\downarrow(\bar{x}_p) \leftarrow \Phi_i^\downarrow(\bar{x}_p) + \Theta_i^\downarrow(\bar{x}_i)$ 
16    PASS2 (index  $i$ )
17     $\triangleright$  Computes  $\Phi_i^\uparrow$  and  $\Phi_i^\circ$ .
18    foreach value  $\bar{x}_i$  of the join attributes  $\bar{X}_i$  of  $S_i$  do
19      if  $S_i$  is not the root of  $\tau$  then
20         $\triangleright$  let  $\bar{x}_p$  be the projection of  $\bar{x}_i$  onto the join attributes shared by
           $S_i$  and its parent in  $\tau$ 
21         $\text{UP\_COUNT} \leftarrow \Phi_i^\uparrow(\bar{x}_p)$ 
22      else
23         $\text{UP\_COUNT} \leftarrow 1$ 
24       $\text{FULL\_JOIN\_SIZE}_i(\bar{x}_i) \leftarrow \Theta_i^\downarrow(\bar{x}_i) \cdot \text{UP\_COUNT}$ 
25      foreach child  $S_j$  of  $S_i$  in  $\tau$  do
26         $\triangleright$  let  $\bar{x}_{ij}$  be the projection of  $\bar{x}_i$  onto  $\bar{X}_{ij}$ 
27         $\Phi_j^\uparrow(\bar{x}_{ij}) \leftarrow \Phi_j^\uparrow(\bar{x}_{ij}) + \text{FULL\_JOIN\_SIZE}_i(\bar{x}_i)$ 
28       $\Phi_i^\circ(\bar{x}_i) \leftarrow \frac{\text{FULL\_JOIN\_SIZE}_i(\bar{x}_i)}{\text{ROWS\_PER\_KEY}_i(\bar{x}_i)}$ 
29      foreach child  $S_j$  of  $S_i$  in  $\tau$  do
30        foreach value  $\bar{x}_{ij}$  of join attributes  $\bar{X}_{ij}$  of  $S_j$  do
31           $\Phi_j^\uparrow(\bar{x}_{ij}) \leftarrow \frac{\Phi_i^\circ(\bar{x}_i)}{\Phi_j^\downarrow(\bar{x}_{ij})}$ 
32    PASS2( $j$ )

```

then $\Phi_i^\circ = \Phi_i^\uparrow$ by definition. For a non-leaf S_i , we re-use the values $\text{FULL_JOIN_SIZE}_i(\bar{x}_i)$ defined above. This value is very similar to $\Phi_i^\circ(\bar{x}_i)$, but also depends on the size $\text{ROWS_PER_KEY}_i(\bar{x}_i)$. We use the equality $\Phi_i^\circ(\bar{x}_i) = \text{FULL_JOIN_SIZE}_i(\bar{x}_i) / \text{ROWS_PER_KEY}_i(\bar{x}_i)$.

Algorithm 1 gives the procedure COMPUTE-COUNTS for shared computation of the three aggregate types. First, in a bottom-up pass of the join tree τ , the aggregates Θ_i^\downarrow and Φ_i^\downarrow are computed. Then, Φ_i^\uparrow and Φ_i° are computed in a top-down pass over τ . The auxiliary view FULL_JOIN_SIZE_i is defined depending on whether S_i is the root. For

every child S_j , the value FULL_JOIN_SIZE_i is added to $\Phi_j^\uparrow(\bar{x}_{ij})$. The division by $\Phi_j^\downarrow(\bar{x}_{ij})$ is done just before the recursive call. Before that call, Φ_i° is computed.

LEMMA 5.1. *Given the matrices S_1, \dots, S_r and the join tree τ , the aggregates $\Phi_i^\downarrow, \Phi_i^\uparrow$ and Φ_i° from Figure 3 can be computed in time $O(|S_1| + \dots + |S_r|)$ and with two passes over these matrices.*

We parallelize Algorithm 1 by executing the loops starting in lines 7 and 15 in parallel for different values \bar{x}_i . Atomic operations are used for the assignments in lines 13 and 22 to handle concurrent write operations of different threads.

6 FIGARO: PUSHING ROTATIONS PAST JOINS

We are now ready to introduce FiGARo. Algorithm 2 gives its pseudocode. It takes as input the matrices S_1, \dots, S_r and a join tree τ of the natural join of the input matrices. It computes an almost upper-triangular matrix \mathbf{R}_0 with at most $|S_1| + \dots + |S_r|$ non-zero rows such that \mathbf{R}_0 can be alternatively obtained from the natural join of the input matrices by a sequence of Givens rotations. It does so in linear time in the size of the input matrices. In contrast to the example in Section 4, FiGARo does not require the join output \mathbf{A} to be materialized. Instead, it traverses the input join tree bottom-up and computes heads and tails of the join of the matrices under each node in the join tree.

FiGARo uses the following two high-level ideas.

First, the join output typically contains multiple copies of an input row, where the precise number of copies depends on the number of rows from other matrices that share the same join key. When using Givens rotations to set all but the first occurrence of a value to zero, this first occurrence will be scaled by some factor, which is given by a count query (Section 5). FiGARo applies the scaling factor directly to the value, without the detour of constructing the multiple copies and getting rid of them again.

Second, all matrix head and tail computations can be done independently on the different columns of the input matrix. FiGARo performs them on the input matrix, where these columns originate, and combines the results, including the application of scaling factors, in a bottom-up pass over the join tree τ .

The algorithm. We now explain the details of FiGARo. It manages two matrices **Data** and **Out**. The matrix **Out** holds the result of FiGARo, the matrix **Data** holds (generalized) heads that will be processed further in later steps. The algorithm proceeds recursively along the join tree τ , starting from the root. It maintains the invariant that after the computation finished for a non-root node S_i of the join tree, **Data** contains exactly one row for every value of the join attributes that are shared between S_i and its parent in τ .

For a matrix S_i , FiGARo first iterates over all values \bar{x}_i of its join attributes \bar{X}_i . For each \bar{x}_i it computes head and tail of the matrix $S_i^{\bar{x}_i}$ that is obtained by selecting all rows of S_i that have the join key \bar{x}_i and then by projecting these rows onto the data columns \bar{Y}_i . The tail is multiplied with the scaling factor $\Phi_i^\circ(\bar{x}_i)$ and written to the output **Out**, adding zeros for other columns. The head is stored in the matrix **Data**. The scaling factor $\sqrt{|S_i^{\bar{x}_i}|}$ that, as to Lemma 3.3, would be applied to other columns, is stored in the vector **scales**. If S_i is a leaf in the join tree τ , then the invariant is satisfied.

Algorithm 2: FiGARo computes the almost upper-triangular matrix \mathbf{R}_0 from the input matrices $\mathbf{S}_1, \dots, \mathbf{S}_m$ with join tree τ .

```

1  FiGARo (input matrices  $\mathbf{S}_1, \dots, \mathbf{S}_r$ , join tree  $\tau$ , index  $i$ )
    $\triangleright$  Out, Data are matrices, scales is a vector. All are initially empty.
2  HEADS_AND_TAILS
3  if  $S_i$  is not a leaf in  $\tau$  then
4    PROCESS_AND_JOIN_CHILDREN
5    if  $S_i$  is not the root of  $\tau$  then
6      PROJECT_AWAY_JOIN_ATTRIBUTES
7    if  $S_i$  is the root of  $\tau$  then
8      Out.APPEND(Data)
9      return Out
10   return (Out, Data, scales)
11 HEADS_AND_TAILS:
    $\triangleright$  Compute heads and tails of  $S_i$ , grouped by the columns  $\bar{X}_i$ . Heads
   are written to Data, tails are scaled and written to Out.
12 foreach value  $\bar{x}_i$  of the join attributes  $\bar{X}_i$  in  $S_i$  do
    $\triangleright$  Let  $S_i^{\bar{x}_i}$  consist of all rows of  $S_i$  with value  $\bar{x}_i$  for columns  $\bar{X}_i$ ,
   projected onto the data attributes  $\bar{Y}_i$ 
13   Out.APPEND( $[T_1 \ \dots \ T_r]$ )
14    $\triangleright$  where  $T_k = \mathbf{0}$  for  $k \neq i$  and  $T_i = \mathcal{T}(S_i^{\bar{x}_i}) \cdot \sqrt{\Phi_i^o(\bar{x}_i)}$ 
15   Data $[\bar{x}_i : \bar{Y}_i] \leftarrow \mathcal{H}(S_i^{\bar{x}_i})$ 
16   scales $[\bar{x}_i] \leftarrow \sqrt{|S_i^{\bar{x}_i}|}$ 
17 PROCESS_AND_JOIN_CHILDREN:
    $\triangleright$  Recursively applies FiGARo to all children. Concatenates the
   results Out, joins the matrices Data and applies the factors scales
18 foreach child  $S_j$  of  $S_i$  in  $\tau$  do
19   (Out $_j$ , Data $_j$ , scales $_j$ )  $\leftarrow$  FiGARo( $\mathbf{S}_1, \dots, \mathbf{S}_r, \tau, j$ )
20   Out.APPEND(Out $_j$ )
21 foreach value  $\bar{x}_i$  of the join attributes  $\bar{X}_i$  in  $S_i$  do
    $\triangleright$  let  $\bar{X}_{ij}$  be the join attributes shared between  $S_i$  and  $S_j$  and let
    $\bar{x}_{ij}$  be the projection of  $\bar{x}_i$  onto  $\bar{X}_{ij}$ .
22   foreach child  $S_j$  of  $S_i$  in  $\tau$  do
23     foreach  $S_k$  in the subtree of  $S_j$  in  $\tau$  do
24       Data $[\bar{x}_i : \bar{Y}_k] \leftarrow$ 
          $\mathbf{Data}_j[\bar{x}_{ij} : \bar{Y}_k] \cdot \mathbf{scales}[\bar{x}_i] \cdot \prod_{j' \in [r] \setminus \{j\}} \mathbf{scales}_{j'}[\bar{x}_{ij}']$ 
25       Data $[\bar{x}_i : \bar{Y}_i] \leftarrow \mathbf{Data}[\bar{x}_i : \bar{Y}_i] \cdot \prod_{j \in [r]} \mathbf{scales}_j[\bar{x}_{ij}]$ 
26       scales $[\bar{x}_i] \leftarrow \mathbf{scales}[\bar{x}_i] \cdot \prod_{j \in [r]} \mathbf{scales}_j[\bar{x}_{ij}]$ 
27 PROJECT_AWAY_JOIN_ATTRIBUTES:
    $\triangleright$  Let  $\bar{X}_p$  be the join attributes shared between  $S_i$  and its parent in  $\tau$ .
   So far, Data has one row for every value of  $\bar{X}_i$ . Reduce this to one
   row for every value of  $\bar{X}_p$ .
28 foreach value  $\bar{x}_p$  of the join attributes  $\bar{X}_p$  in  $S_i$  do
29   Out.APPEND( $[T_1 \ \dots \ T_r]$ )
30    $\triangleright$  where  $T_k = \mathbf{0}$  if  $S_k$  is not in the subtree of  $S_i$  in  $\tau$ ; else
31    $T_k = \mathcal{T}(\mathbf{Data}[\bar{x}_p, * : \bar{Y}_k], \mathbf{scales}[\bar{x}_p, *]) \cdot \sqrt{\Phi_i^\uparrow(\bar{x}_p)}$ 
32   Data' $[\bar{x}_p :] \leftarrow \mathcal{H}(\mathbf{Data}[\bar{x}_p, * :], \mathbf{scales}[\bar{x}_p, *])$ 
33   scales' $[\bar{x}_p] \leftarrow \sqrt{\Phi_i^\downarrow(\bar{x}_p)}$ 
34   (Data, scales)  $\leftarrow$  (Data', scales')

```

If S_i is not a leaf in the join tree τ , then the algorithm is recursively called for its children. Any output of the recursive calls is written to **Out**. The recursive call for the child S_j also returns a matrix **Data** $_j$ that contains columns \bar{Y}_k with computed heads corresponding to this column, for all k such that S_k is in the subtree of S_j in τ , as well as scaling factors **scales** $_j$. As to the maintained invariant, **Data** $_j$ contains exactly one row for every value of the join attributes \bar{X}_{ij} that are shared between S_i and S_j .

The contents of the matrices **Data** and **Data** $_j$ are joined. More precisely, for each join value \bar{x}_i of the attributes \bar{X}_i of S_i , the entry **Data** $[\bar{x}_i : \bar{Y}_k]$ is set to the entry **Data** $_j[\bar{x}_{ij} : \bar{Y}_k]$, where \bar{x}_{ij} is the projection of \bar{x}_i onto \bar{X}_{ij} . Also, scaling factors are applied to the different columns of **Data**. For the columns \bar{Y}_k , all scaling factors from **scales** and from the vectors **scales** $_j$ need to be applied, for all j such that S_k is not in the subtree of S_j . In the case of \bar{Y}_i , all factors from the vectors **scales** $_j$ are applied, but not from **scales**.

If S_i is not the root of the join tree then rows of **Data** are aggregated in PROJECT_AWAY_JOIN_ATTRIBUTES to satisfy the invariant. Before entering the loop of Line 28, **Data** contains one row for every value \bar{x}_i of the join attributes \bar{X}_i of S_i . The number of rows is reduced in PROJECT_AWAY_JOIN_ATTRIBUTES such that there is only one row for every value \bar{x}_p of the join attributes \bar{X}_p that are shared between S_i and its parent in τ . To do so, FiGARo iterates over all values \bar{x}_p of these attributes. For each \bar{x}_p it takes the rows of **Data** for the keys \bar{x}_i that agree with \bar{x}_p on \bar{X}_p , and computes their generalized head and tail. The generalized tail is scaled by the factor $\sqrt{\Phi_i^\uparrow(\bar{x}_p)}$ and written to **Out**, adding zeros for other columns. The matrix **Data** is overwritten with the collected generalized heads. So, the invariant is satisfied now. The scaling factor $\sqrt{\Phi_i^\downarrow(\bar{x}_p)}$ equals the scaling factor that is applied to other columns as per Lemma 3.5, and is stored.

The next theorem states that indeed the result of FiGARo is an almost upper-triangular matrix with a linear number of non-zero rows. It also states the runtime guarantees of FiGARo.

THEOREM 6.1. *Let the matrices $\mathbf{S}_1, \dots, \mathbf{S}_r$ represent fully reduced relations and let τ be any join tree of the natural join over these relations. Let A be the matrix representing this natural join. Let M be the overall number of rows and N be the overall number of data columns in the input matrices S_i .*

On input $(\mathbf{S}_1, \dots, \mathbf{S}_r, \tau, 1)$, FiGARo returns in $O(MN)$ time a matrix \mathbf{R}_0 such that:

- (1) \mathbf{R}_0 has at most M rows,
- (2) there is an orthogonal matrix \mathbf{Q} such that $A[:, \bar{Y}] = \mathbf{Q} \begin{bmatrix} \mathbf{R}_0 \\ \mathbf{0} \end{bmatrix}$.

We can parallelize FiGARo by executing the loop starting in line 12 of Algorithm 2 in parallel for different values \bar{x}_i , similarly for the loops starting in lines 28 and 21. As the executions are independent, no synchronization between the threads is necessary.

Comparison with Section 4. We exemplify the execution of FiGARo using the same input as in Section 4, which is depicted in Figure 2. We will obtain the same result \mathbf{R}_0 as in that section, modulo permutations of rows.

After the initial call of FiGARo($\mathbf{S}_1, \dots, \mathbf{S}_4, \tau, 1$), at first heads and tails of S_1 are computed. We skip the explanation of this part and focus on the following recursive call of FiGARo($\mathbf{S}_1, \dots, \mathbf{S}_4, \tau, 2$).

When computing the heads and tails of S_2 , at first the matrices $\sqrt{\Phi_2^\circ(a_j b_k c_\ell)} \mathcal{T}(S_2^{a_j b_k c_\ell})$ are padded with zeros and written to **Out**, for all $j, k, \ell \in \{1, 2\}$. Then, **Data** $[a_j b_k c_\ell : Y_3]$ is set to $\mathcal{H}(S_2^{a_j b_k c_\ell})$ and **scales** $[a_j b_k c_\ell]$ becomes $\sqrt{|S_2^{a_j b_k c_\ell}|}$.

Next, the children S_3 and S_4 of S_2 in τ are processed and the intermediate results are joined. The recursive calls for the children return **Data** $_3[b_k : Y_3] = \mathcal{H}(S_3^{b_k})$ and **scales** $_3[b_k] = \sqrt{|S_3^{b_k}|}$ as well as **Data** $_4[c_\ell : Y_4] = \mathcal{H}(S_4^{c_\ell})$ and **scales** $_4[c_\ell] = \sqrt{|S_4^{c_\ell}|}$, plus the matrices **Out** $_3$, **Out** $_4$ that contain as non-zero entries $\sqrt{\Phi_3^\circ(b_k)} \mathcal{T}(S_3^{b_k})$ and $\sqrt{\Phi_4^\circ(c_\ell)} \mathcal{T}(S_4^{c_\ell})$, respectively, for every $k, \ell \in \{1, 2\}$.

After joining the results and applying the scaling factors, the rows **Data** $[a_j b_k c_\ell :]$ are as follows for every $j, k, \ell \in \{1, 2\}$, where we use $\beta_{jk\ell} = \sqrt{|S_2^{a_j b_k c_\ell}| \cdot |S_3^{b_k}| \cdot |S_4^{c_\ell}|}$:

$$\begin{array}{ccc} Y_2 & Y_3 & Y_4 \\ \frac{\beta_{jk\ell}}{\sqrt{|S_2^{a_j b_k c_\ell}|}} \mathcal{H}(S_2^{a_j b_k c_\ell}) & \frac{\beta_{jk\ell}}{\sqrt{|S_3^{b_k}|}} \mathcal{H}(S_3^{b_k}) & \frac{\beta_{jk\ell}}{\sqrt{|S_4^{c_\ell}|}} \mathcal{H}(S_4^{c_\ell}) \end{array}$$

It holds **scales** $[a_j b_k c_\ell] = \beta_{jk\ell}$.

Notice the similarity to the corresponding rows from Section 4, where, for $j = 1$ and $\alpha_{k\ell} = \sqrt{|S_1^{a_1}| \cdot |S_2^{a_1 b_k c_\ell}| \cdot |S_3^{b_k}| \cdot |S_4^{c_\ell}|}$, we obtained the rows

$$\begin{array}{ccc} Y_1 & Y_2 & Y_3 & Y_4 \\ \frac{\alpha_{k\ell}}{\sqrt{|S_1^{a_1}|}} \mathcal{H}(S_1^{a_1}) & \frac{\alpha_{k\ell}}{\sqrt{|S_2^{a_1 b_k c_\ell}|}} \mathcal{H}(S_2^{a_1 b_k c_\ell}) & \frac{\alpha_{k\ell}}{\sqrt{|S_3^{b_k}|}} \mathcal{H}(S_3^{b_k}) & \frac{\alpha_{k\ell}}{\sqrt{|S_4^{c_\ell}|}} \mathcal{H}(S_4^{c_\ell}). \end{array}$$

For $j = 1$, the only difference in the columns Y_2 to Y_4 is in the scaling factors $\alpha_{k\ell}$ and $\beta_{1k\ell}$, which only differ by the factor $\sqrt{|S_1^{a_1}|}$.

The join attributes X_{23} and X_{24} are then projected away, as they do not appear in the parent S_1 of S_2 . Observe that the vectors that are used for defining the generalized heads and tails are the same here and in Section 4. For example, the part of **scales** that corresponds

to $a_j = a_1$ is equal to the vector $\mathbf{v} = \begin{bmatrix} \sqrt{|S_2^{a_1 b_1 c_1}| \cdot |S_3^{b_1}| \cdot |S_4^{c_1}|} \\ \vdots \\ \sqrt{|S_2^{a_1 b_2 c_2}| \cdot |S_3^{b_2}| \cdot |S_4^{c_2}|} \end{bmatrix}$ that

was used in Section 4. So, the generalized heads and tails for the rows of **Data** associated with join keys a_1 and a_2 , respectively, have the same results as in Section 4 for the columns Y_2 to Y_4 , modulo the factor $\sqrt{|S_1^{a_1}|}$. This factor equals $\sqrt{\Phi_2^\uparrow(a_1)}$, which FiGARo applies to the generalized tails. The factor is also applied to the generalized heads in **Data** after the call of FiGARo for S_2 terminates, by **PROCESS_AND_JOIN_CHILDREN** in the call **FiGARo**($S_1, \dots, S_4, \tau, 1$). There, also the column Y_1 is added. The rows in the final result of the call **FiGARo**($S_1, \dots, S_4, \tau, 1$) are then the same as in Section 4.

7 POST-PROCESSING

The output of FiGARo is so far not the upper-triangular matrix **R** but a matrix **R** $_0$ that consists of linearly many rows in the size of the input matrices. The transformation of **R** $_0$ into **R** is the task of a post-processing step that we describe in this section. This step can be achieved by general techniques for QR factorization, such

as Householder transformations and textbook Givens rotations approaches. The approach we present here exploits the structure of **R** $_0$, which has large blocks of zeros.

The non-zero blocks of **R** $_0$ are either tails of matrices (see line 13 of Algorithm 2), generalized tails of sets of matrices (line 29), or the content of the matrix **Data** at the end of the execution of FiGARo (line 8). In a first post-processing step, these blocks are upper-triangularized individually and potentially arising all-zero rows are discarded. In a second post-processing step, the block of resulting rows is made upper-triangular, leading to the matrix **R**.

In both steps we need to make blocks of rows upper-triangular, i.e., we need to compute their QR decomposition. This can be done using off-the-shelf Householder transformations. We implemented an alternative method dubbed THIN [12, 20]. It first divides the rows of a block among the available threads, each thread then applies a sequence of Givens rotations to bring its share of rows into upper-triangular form. Then THIN uses a classical parallel Givens rotations approach [21, p. 257] on the collected intermediate results to obtain the final upper-triangular matrix.

All approaches need time $O(MN^2)$, where M is the number of rows and N is the number of columns of the input **R** $_0$ to post-processing. While the main part of FiGARo works in linear time in the overall number of rows and columns of the input matrices (Theorem 6.1), post-processing is only linear in the number of rows.

8 EXPERIMENTS

We benchmarked runtime performance and accuracy of FiGARo against: openblas 0.13.3 called from numpy 1.22.0 built from source; MKL 2021.2.0 using the MKL C++ API (MKL called from numpy is slower); and our post-processing THIN as surrogate for applying FiGARo to the materialized join. MKL and openblas implement the Householder algorithm for the QR decomposition of dense matrices [24]. FiGARo is the only system working on the input datasets, all others work on the materialized join. The engines FiGARo-THIN and FiGARo-MKL are FiGARo followed by THIN and MKL post-processing, respectively. FiGARo and THIN use row-major order for storing matrices, while MKL uses column-major order; we verified that they perform best for their respective orders.

All systems compute the upper-triangular matrix **R**, the orthogonal matrix **Q** is not computed in the following experiments. We verified experimentally that computing the orthogonal matrix **Q** on our three datasets as **AR** $^{-1}$ without materializing **A** [10] is in average 1.5x faster than MKL, which uses the already materialized **A** and internal hints from the prior computation of **R**.

We show that FiGARo outperforms the competitors in both accuracy and runtime performance by a factor proportional to the gap between the join output and input sizes. This factor is up to two orders of magnitude in our experiments. This includes scenarios with key - fkey joins over real data with millions of rows and tens of data columns and with many-to-many joins over synthetic data with thousands of rows and columns. Whenever the join input and output sizes are very close, however, FiGARo's benefit is small; we verify this by reducing the number of rows and increasing the number of columns of our real data. When the number of data columns is at least the square root of the number of rows, e.g., 1K columns and 1M rows in our experiments, the performance gap

	Retailer	Favorita	Yelp
Input Database			
# rows (M)	86 / 0.84	125 / 1.28	2 / 0.02
size on disk (GB)	7.9 / 39	15 / 49	0.53 / 0.075
Join Result			
# rows (M)	84 / 0.84	127 / 1.27	150 / 1.5
# data columns	43 / 2005	30 / 1645	50 / 391
size on disk (GB)	85 / 40	90 / 50	176 / 14
PSQL compute time (sec)	172.67 / 0.74	177.77 / 0.82	180.81 / 1.53

Table 1: Characteristics of used real datasets. There are two numbers in each cell, one for the default dataset and the second for its one-hot encoded version.

almost vanishes – this is to be expected, since the complexity of computing the upper-triangular matrix increases linearly with the number of rows and quadratically with the number of columns.

Experimental Setup. All experiments were performed on an Intel Xeon Silver 4214 (24 physical/48 logical cores, 1GHz, 188GiB) with Debian GNU/Linux 10. We use g++ 10.1 for compiling the generated C++ code using the O3 optimization flag. The performance numbers are averages over 20 consecutive runs. We do not consider the time to load the database into RAM and assume that all relations and the join are sorted by their join attributes.

Datasets. We use three real datasets. Retailer [37] and Favorita [15] are used for forecasting user demands and sales. Yelp [44] has review ratings given by users to businesses. The characteristics of these datasets (Table 1) are common in retail and advertising, where data is generated by sales transactions or click streams.

Retailer has a snowflake schema, Favorita has a star schema. Both have key - fkey joins, a large fact table, and several small dimension tables. Yelp has a star schema with many-to-many joins. We also consider an OHE version of 1% of these datasets, where some keys are one-hot encoded in the data column space. They yield wider matrices to stress-test the decomposition algorithms. Some plots show performance as function of a percentage of the join over the dataset. The corresponding reduced dataset is computed by projecting the join fragment onto the schemas of the relations. When taking a percentage of an OHE dataset, we map an attribute domain to that percentage of it using division hashing.

We also use synthetic datasets consisting of two relations $S, T \in \mathbb{R}^{m \times n}$, whose join is the Cartesian product. For performance experiments, the data in each column follows a uniform distribution in the range $[-3, 3]$. For accuracy experiments, we fix (part of) the output R_{fixed} and derive the input relation S so that the QR decomposition of the Cartesian product agrees with R_{fixed} . The advantage of this approach is that R_{fixed} can be effectively used as ground truth for checking the accuracy of the algorithms.

Experiment 1: Runtime performance. When compared to its competitors, FiGaRo performs very well for real data in case the join output is larger than its input. Figure 4 (top) gives the runtime performance of FiGaRo-THIN, THIN, and MKL for the three real datasets as a function of the percentage of the dataset. The performance gap remains mostly unchanged as the data size is increased. Relative to MKL, FiGaRo-THIN is 2.9x faster for Retailer, 16.1x for Favorita and 120.5x for Yelp. MKL outperforms THIN, except for Favorita where the latter is 4.3x faster than the former. This is because Favorita has the smallest number of columns amongst the

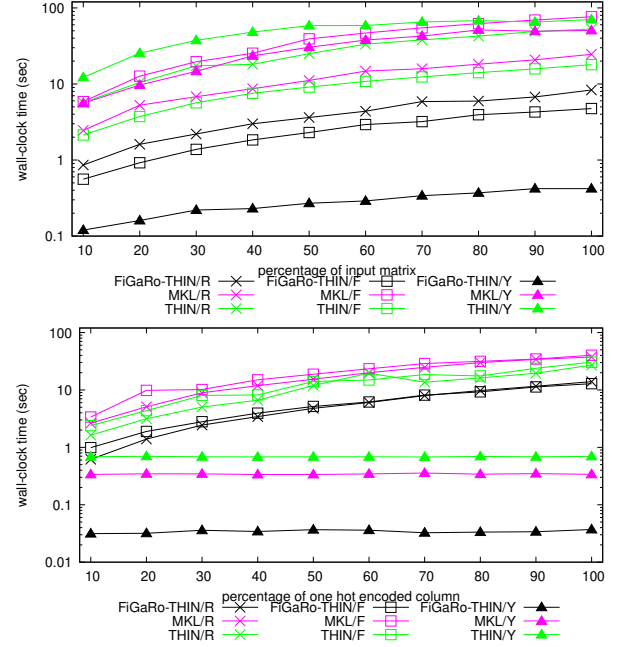


Figure 4: Experiment 1: Runtime performance of FiGaRo and MKL for Retailer (R), Favorita (F), and Yelp (Y). Top: Real datasets. Bottom: OHE data versions.

three datasets and THIN works particularly well on thin matrices. FiGaRo-MKL is not shown to avoid clutter; it consistently performs worse (up to 3x) than FiGaRo-THIN.

We next consider the OHE versions of Retailer and Favorita, for which the join input and output are close. Figure 4 (bottom) gives the runtime performance of FiGaRo-THIN, THIN, and MKL for the one-hot encoded fragments of the three real datasets as a function of the percentage of one-hot encoded columns. FiGaRo’s strategy to push past joins is less beneficial in this case, as it copies heads and tails along the join tree without a significant optimization benefit. Relative to MKL, it is 2.7x faster for Retailer and 3.1x faster for Favorita. The explanation for this speed-up is elsewhere: Whereas the speed-up in Figure 4 (top) is due to structural sparsity, as enforced by the joins, here we have value sparsity due to the many zeros introduced by one-hot encoding. By sorting on the one-hot encoded attribute and allocating blocks with the same attribute value to each thread, we ensure that large blocks of zeros in the one-hot encoding will not be dirtied by the rotations performed by the thread. This effectively preserves many zeros from the input and reduces the number of rotations needed in post-processing to zero values in the output of FiGaRo. This strategy needs however to be supported by a good join tree: A relation with one-hot encoded attributes is sorted on these attributes and this order is a prefix of the sorting order used by its join with its parent relation in the join tree.

We further verified that more input rows allowed FiGaRo to scale better, but MKL ran out of memory. THIN and MKL have similar performance. For the Yelp OHE dataset, its size remains much less than its join result and FiGaRo outperforms MKL by 9x.

Pronounced benefits are obtained for many-to-many joins, for which the join output is much larger than the input. We verified this

#rows	#columns				#columns	#columns	#columns	#columns
	2 ⁶	2 ⁸	2 ¹⁰	2 ¹²	2 ⁶	2 ⁸	2 ¹⁰	2 ¹²
2 ⁹	0.10	0.13	0.17	0.43	3	18	104	368
2 ¹⁰	0.10	0.13	0.30	0.81	16	76	246	609
2 ¹¹	0.12	0.15	0.31	1.77	53	278	785	
2 ¹²	0.12	0.14	0.38	4.65	201	1056		
2 ¹³	0.13	0.18	0.54	5.85	672			

Figure 5: Experiment 1: Runtime performance of FiGARo-MKL and MKL on the Cartesian product of two relations. The reported numbers of rows and columns are (per relation): for 2¹² columns and 2¹³ rows, MKL’s input matrix has 2¹³ columns and 2²⁶ rows. Left: Runtime performance of FiGARo-MKL (seconds). Right: speed-up of FiGARo-MKL over MKL (rounded to closest natural number). An empty cell means that MKL run out of memory.

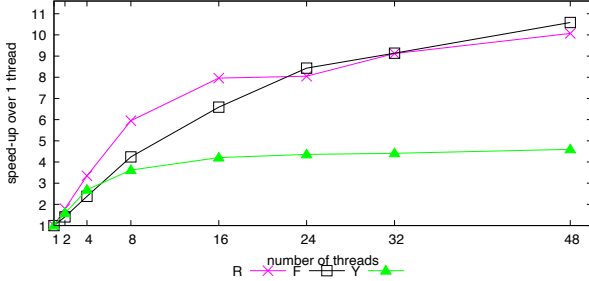


Figure 6: Experiment 2: Multi-threaded FiGARo-THIN speed-up over FiGARo-THIN for one thread for Retailer (R), Favorita (F), and Yelp (Y).

claim using Cartesian products of two relations of thousands of rows and columns. FiGARo outperforms MKL by up to three orders of magnitude on such synthetic data (Figure 5). As expected, FiGARo scales linearly with the number of rows. In contrast, MKL scales quadratically since it works on the materialized Cartesian product. The speed-up of FiGARo over MKL increases as we increase the number of rows and columns of the two input relations. For wide relations (2¹² columns), FiGARo-MKL (shown in figure) is up to 10x faster than FiGARo-THIN (not shown).

In this first experiment, most of the time for FiGARo is taken by post-processing. Computing the batch of the group-by aggregates and the tails and heads of the input relations are much optimized and take under 10% of the overall time for OHE datasets, and about 50% for the original datasets. For FiGARo, we report the time to compute both **R** and the join *intertwined*, whereas for the competitors we only report the time to compute **R**. Table 1 gives the join times for the three datasets; these join times are larger than the MKL compute times. Openblas is 1.5-5 times slower than MKL and not shown. All engines use all cores in this experiment.

Experiment 2: FiGARo on multi-cores. Figure 6 shows the performance of FiGARo-THIN for the three real datasets as we vary the number of threads up to the number of available logical cores (48). The fastest speed-up increase is achieved up to 8 threads for all datasets and up to 16 threads for Retailer and Favorita. The speed-up still increases up to 48 threads, yet its slope gets smaller.

	Retailer	Favorita	Yelp
Original	Bad I(L(C), W, T) 67.10s	S(T, (R, O), H, I)) 29.34s	R(B(C, I, H), U) 1.31s
	Good L(C, I(W, T)) 8.06x	R(T(O, S(H, I))) 6.17x	B(C, I, H, R(U)) 3.13x
OHE	Bad L(C, I (W, T)) 431.57s	H(S (T(R, O), I)) 802.62s	B(C, I, H, R (U))) 11.91s
	Good T(I (L(C), W)) 21.25x	I (S(T(R, O), H)) 47.13x	U(R (B(C, I, H))) 394.07x

Table 2: Experiment 3: FiGARo-THIN’s runtime for a bad join tree and relative speed-up for a good one. The join trees are written in term notation over the abbreviated relation names: Retailer: Inventory(I), Item(T), Weather(W), Location(L), Census(C); Favorita: Sales(S), Stores(R), Oil(O), Holidays(H), Items(I), Transactions(T); Yelp: Business(B), Category(C), CheckIn(I), Review(R), User (U), Hours(H). The relation with one-hot encoded values is marked in red.

This is in particular the case for the smallest dataset Yelp, for which FiGARo-THIN already takes under 0.5 seconds using 8 threads. FiGARo uses domain parallelism: It splits each input relation into as many contiguous blocks as available threads and applies the same transformation to each block independently.

Experiment 3: Effect of join trees. Different join trees may lead to different runtimes for FiGARo. As in classical query optimization, FiGARo prefers join trees such that overall size of the intermediate results is the smallest. For our datasets, this translates to having the large fact tables involved earlier in the joins. We explain for Retailer, whose large and narrow fact table Inventory uses key - fkey joins on composite keys (item id, date, location) to join with the small dimension tables Locations, Weather, Item and Census. FiGARo aggregates away join keys as it moves from leaves to the root of the join tree. By aggregating away join keys over the large table as soon as possible, it creates small intermediate results and reduces the number of copies of dimension-table tuples in the intermediate results to pair with tuples in the fact table. If the fact table would be the root, then FiGARo would first join it with its children in the join tree and then apply transformations, with no benefit over MKL as in both cases we would work on the materialized join output. Therefore, a bad join tree for Retailer therefore has Inventory (I) as root. In contrast, a good join tree first joins Inventory with Weather and Item, thereby aggregating away the item id and date keys and to reduce the size of the intermediate result to be joined with Census and Location. As shown in Table 2, FiGARo-THIN performs 8.06x faster using a good join tree instead of a bad one.

For the OHE datasets, a key performance differentiator is the sorting order of the relations with one-hot encoded attributes, as explained in Experiment 1. For instance, the relation Inventory in the Retailer dataset (colored red in Table 2) has the one-hot encoded attribute product id. In a bad join tree, it is not sorted on this attribute: it joins with its parent relation Location on location id, so it is primarily sorted on location id. In a good join tree, Inventory is sorted on product id as it joins with its parent Item on product id.

Experiment 4: Accuracy. For this experiment we use a synthetic dataset consisting of two relations with an exponentially increasing number of rows and columns. Their join is the Cartesian product. The input relations are defined based on a given matrix R_{fixed} such

#rows	#columns			#columns		
	2 ⁴	2 ⁶	2 ⁸	2 ⁴	2 ⁶	2 ⁸
2 ⁹	2.3e-15	1.8e-14	3.7e-14	26	1.5	1.2
2 ¹⁰	3.5e-15	3.3e-14	1.3e-13	73	5.3	1.3
2 ¹¹	4.7e-15	4.3e-14	3.2e-13	250	20	1.6
2 ¹²	6e-15	5.4e-14	5.2e-13	830	64	5.4
2 ¹³	7.9e-15	6.3e-14		2600	250	

Table 3: Experiment 4: (Left) Error for FiGARo-MKL relative to the ground truth. (Right) Division of relative error of MKL over relative error of FiGARo-MKL. The empty bottom-right cell is due to out-of-memory error for MKL.

that \mathbf{R}_{fixed} is part of the upper-triangular factor \mathbf{R} of the QR decomposition. The error of an algorithm is given by the relative error $\frac{\|\mathbf{R}_{fixed} - \hat{\mathbf{R}}_{fixed}\|_F}{\|\mathbf{R}_{fixed}\|_F}$ of the computed partial result $\hat{\mathbf{R}}_{fixed}$ compared to the ground truth \mathbf{R}_{fixed} , where $\|\cdot\|_F$ is the Frobenius norm.

Table 3 (left) shows the error of FiGARo-MKL. As the number of rows increases, the accuracy only changes slightly. The accuracy drops as the number of columns increases. The error remains however sufficiently close to the machine representation unit (10^{-16}). We also verified that FiGARo-THIN’s error is very similar.

We also computed the relative error for MKL. Table 3 (right) shows the result of dividing the relative errors of MKL and FiGARo-MKL. A number greater than 1 means that FiGARo-MKL is more accurate than MKL. The error gap increases with the number of rows and decreases with the number of columns. The latter is as expected, as post-processing dominates the computation for wide matrices. As shown in the table, FiGARo-MKL is up to three orders of magnitude more accurate than MKL.

9 RELATED WORK

Our work is the first to investigate the Givens QR decomposition over database joins. It complements seminal seven-decades-old work on QR decomposition and is part of an on-going effort at the interface of linear algebra and databases. Our motivation for this work is the emergence of machine learning algorithms and applications, which build on linear algebra, over relational data.

Improving performance of linear algebra operations. Factorized data computation [33] is a paradigm that uses structural compression to lower the cost of computing a variety of database and machine learning workloads. It has been used for the efficient computation of $\mathbf{A}^T \mathbf{A}$ over training datasets \mathbf{A} created by feature extraction queries, as used for learning a variety of linear and non-linear regression models [26, 28, 31, 36, 37]. It is also used for fundamental linear algebra operations, such as matrix multiplication and element-wise matrix and scalar operations [10]. Besides structural compression, also value-based compression is useful for fast in-memory matrix-vector multiplication [14]. Existing techniques for matrix multiplication, as supported by open-source systems like SystemML [8], Spark [46], and Julia [3], exploit the sparsity of the matrices. This calls for sparsity estimation in the form of zeroes [40]. The matrix layout can also have a large impact on the performance of matrix computation in a distributed environment [30]. Distributed and parallel relational database systems that account for the specific workload brought by linear algebra computation [29] may represent an alternative to high performance

computing efforts such as ScaLAPACK [11]. There are distributed algorithms for QR decomposition in ScaLAPACK [9, 42].

QR decomposition. There are three main approaches to QR decomposition. Our work considers *Givens rotations* [19]. Each application of a Givens rotation to a matrix \mathbf{A} sets one entry of \mathbf{A} to 0. This method can be parallelized, as each rotation only affects two rows of \mathbf{A} . It is particularly efficient for sparse matrices. One form of sparsity is the presence of many zeros. We show its efficiency for another form of sparsity: the presence of repeating blocks whose one-off transformation can be reused multiple times.

Householder transformations [24] are particularly efficient for dense matrices [23, p. 366]. MKL and openblas used in our experiments implement this method. One Householder transformation sets all but one entry of a vector to 0, so the QR decomposition of an $m \times n$ matrix can be obtained using n transformations. Both Givens and Householder are numerically stable [23, Chapter 19].

The *Gram-Schmidt process* [22, 38] computes the orthogonal columns of \mathbf{Q} one after another by subtracting iteratively from the i -th column of \mathbf{A} all of its projections onto the 1 to $i - 1$ previously computed orthogonal columns of \mathbf{Q} . A slightly modified variant [5] is numerically stable. The modified Gram-Schmidt is mathematically and numerically equivalent to applying Householder transformations to a matrix that is padded with zeros [6].

Implementing Givens rotations. There are several options on how to set the values c and s of a Givens rotation matrix in the presence of negative values. We follow the choice proposed by Bindel [4]. Anderson [2] defends the original choice [19] of signs using numerical stability arguments. Gentleman [18] shows that one can compute an upper-triangular matrix \mathbf{R}' and a diagonal matrix \mathbf{D} without computing square roots such that $\mathbf{R} = \mathbf{D}^{\frac{1}{2}} \mathbf{R}'$. Stewart [41, p. 291] discusses in depth these fast rotations.

10 CONCLUSION AND FUTURE WORK

This paper introduces FiGARo, an algorithm that computes the QR decomposition of matrices defined by joins over relational data. By pushing the computation past the joins, FiGARo can significantly reduce the number of computation steps. We experimentally verified that FiGARo can outperform in both runtime and accuracy linear algebra packages such as Intel MKL and openblas.

FiGARo’s technique is also applicable to the LU matrix decomposition, where \mathbf{L} is lower-triangular and \mathbf{U} is upper-triangular. Further decompositions, such as SVD and eigenvalue, can be constructed from the result of the QR decomposition.

ACKNOWLEDGMENTS

This project has received funding from the European Union’s Horizon 2020 research and innovation programme under grant agreement No 682588.

REFERENCES

- [1] Serge Abiteboul, Richard Hull, and Victor Vianu. 1995. *Foundations of Databases*. Addison-Wesley, Boston, MA, USA. <http://webdam.inria.fr/Alice/>
- [2] Edward Anderson. 2000. *Discontinuous Plane Rotations and the Symmetric Eigenvalue Problem*. Technical Report 150. LAPACK Working Note.
- [3] Jeff Bezanson, Alan Edelman, Stefan Karpinski, and Viral B. Shah. 2017. Julia: A Fresh Approach to Numerical Computing. *SIAM Rev.* 59, 1 (2017), 65–98.
- [4] David Bindel, James Demmel, William Kahan, and Osni Marques. 2002. On computing givens rotations reliably and efficiently. *ACM Trans. Math. Softw.* 28,

- 2 (2002), 206–238.
- [5] Åke Björck. 1967. Solving linear least squares problems by Gram-Schmidt orthogonalization. *BIT* 7, 1 (1967), 1–21.
 - [6] Åke Björck and Christopher C. Paige. 1992. Loss and Recapture of Orthogonality in the Modified Gram-Schmidt Algorithm. *SIAM J. Matrix Anal. Appl.* 13, 1 (1992), 176–190.
 - [7] Matthias Böhm, Douglas R. Burdick, Alexandre V. Evfimievski, Berthold Reinwald, Frederick R. Reiss, Prithviraj Sen, Shirish Tatikonda, and Yuanyuan Tian. 2014. SystemML’s Optimizer: Plan Generation for Large-Scale Machine Learning Programs. *IEEE Data Eng. Bull.* 37, 3 (2014), 52–62.
 - [8] Matthias Böhm, Douglas R. Burdick, Alexandre V. Evfimievski, Berthold Reinwald, Frederick R. Reiss, Prithviraj Sen, Shirish Tatikonda, and Yuanyuan Tian. 2014. SystemML’s Optimizer: Plan Generation for Large-Scale Machine Learning Programs. *IEEE Data Eng. Bull.* 37, 3 (2014), 52–62.
 - [9] Zvonimir Bujanovic and Zlatko Drmac. 2019. New robust ScaLAPACK routine for computing the QR factorization with column pivoting. *CoRR* abs/1910.05623 (2019).
 - [10] Lingjiao Chen, Arun Kumar, Jeffrey F. Naughton, and Jignesh M. Patel. 2017. Towards Linear Algebra over Normalized Data. *Proc. VLDB Endow.* 10, 11 (2017), 1214–1225.
 - [11] Jaeyoung Choi, James Demmel, Inderjit S. Dhillon, Jack J. Dongarra, Susan Ostrouchov, Antoine Petit, Ken Stanley, David W. Walker, and R. Clinton Whaley. 1995. ScaLAPACK: A Portable Linear Algebra Library for Distributed Memory Computers - Design Issues and Performance. In *Applied Parallel Computing, Computations in Physics, Chemistry and Engineering Science*, Vol. 1041. 95–106.
 - [12] Rudnei Dias da Cunha, Dulcenéia Becker, and James Carlton Patterson. 2002. New parallel (rank-revealing) QR factorization algorithms. In *European Conference on Parallel Processing*. Springer, 677–686.
 - [13] Oksana Dolmatova, Nikolaus Augsten, and Michael H. Böhlen. 2020. A Relational Matrix Algebra and its Implementation in a Column Store. In *SIGMOD*. 2573–2587.
 - [14] Ahmed Elgohary, Matthias Boehm, Peter J. Haas, Frederick R. Reiss, and Berthold Reinwald. 2019. Compressed linear algebra for declarative large-scale machine learning. *Commun. ACM* 62, 5 (2019), 83–91.
 - [15] Corporacion Favorita. 2017. Corp. Favorita Grocery Sales Forecasting: Can you accurately predict sales for a large grocery chain? <https://www.kaggle.com/c/favorita-grocery-sales-forecasting/>.
 - [16] J.G.F. Francis. 1961. The QR Transformation, I. *Comput. J.* 4, 3 (1961), 265–271. received October 1959.
 - [17] Floris Geerts, Thomas Muñoz, Cristian Riveros, and Domagoj Vrgoc. 2021. Expressive Power of Linear Algebra Query Languages. In *PODS*. 342–354.
 - [18] W. Morven Gentleman. 1973. Least Squares Computations by Givens Transformations Without Square Roots. *IMA J. Applied Maths* 12, 3 (1973), 329–336.
 - [19] Wallace Givens. 1958. Computation of Plain Unitary Rotations Transforming a General Matrix to Triangular Form. *J. of Soc. for Industrial and Applied Maths* 6, 1 (1958), 26–50.
 - [20] Gene Howard Golub, Robert J Plemmons, and Ahmed Sameh. 1986. *Parallel block schemes for large scale least squares computations*. Technical Report. Stanford Univ., CA (USA). Dept. of Computer Science; North Carolina State
 - [21] Gene H. Golub and Charles F. Van Loan. 2013. *Matrix Computations* (fourth ed.). The Johns Hopkins University Press.
 - [22] J.P. Gram. 1883. Ueber die Entwicklung reeller Functionen in Reihen mittelst der Methode der kleinsten Quadrate. *Journal für die reine und angewandte Mathematik* 1883, 94 (1883), 41–73.
 - [23] Nicholas J. Higham. 2002. *Accuracy and Stability of Numerical Algorithms* (second ed.). J. of Soc. for Industrial and Applied Maths.
 - [24] Alston S. Householder. 1958. Unitary Triangularization of a Nonsymmetric Matrix. *J. ACM* 5, 4 (1958), 339–342.
 - [25] Dylan Hutchison, Bill Howe, and Dan Suciu. 2017. LaraDB: A Minimalist Kernel for Linear and Relational Algebra Computation. In *BeyondMR@SIGMOD*. 2:1–2:10.
 - [26] Mahmoud Abo Khamis, Hung Q. Ngo, XuanLong Nguyen, Dan Olteanu, and Maximilian Schleich. 2020. Learning Models over Relational Data Using Sparse Tensors and Functional Dependencies. *ACM Trans. Database Syst.* 45, 2 (2020), 7:1–7:66.
 - [27] Mahmoud Abo Khamis, Hung Q. Ngo, and Atri Rudra. 2016. FAQ: Questions Asked Frequently. In *PODS*. 13–28.
 - [28] Side Li, Lingjiao Chen, and Arun Kumar. 2019. Enabling and Optimizing Non-linear Feature Interactions in Factorized Linear Algebra. In *SIGMOD*. 1571–1588.
 - [29] Shangyu Luo, Zekai J. Gao, Michael N. Gubanov, Luis Leopoldo Perez, Dimitrije Jankov, and Christopher M. Jermaine. 2020. Scalable linear algebra on a relational database system. *Commun. ACM* 63, 8 (2020), 93–101.
 - [30] Shangyu Luo, Dimitrije Jankov, Binhang Yuan, and Chris Jermaine. 2021. Automatic Optimization of Matrix Implementations for Distributed Machine Learning and Linear Algebra. In *SIGMOD*. 1222–1234.
 - [31] Dan Olteanu. 2020. The Relational Data Borg is Learning. *Proc. VLDB Endow.* 13, 12 (2020), 3502–3515.
 - [32] Dan Olteanu, Jiewen Huang, and Christoph Koch. 2009. SPROUT: Lazy vs. Eager Query Plans for Tuple-Independent Probabilistic Databases. In *ICDE*. 640–651.
 - [33] Dan Olteanu and Maximilian Schleich. 2016. Factorized Databases. *SIGMOD Rec.* 45, 2 (2016), 5–16.
 - [34] H. Rutishauser. 1958. Solution of eigenvalue problems with the LR-transformation. Further Contributions to the Solution of Simultaneous Linear Equations and the Determination of Eigenvalues. *Applied Mathematics Series. National Bureau of Standards* 49 (1958), 47–81.
 - [35] Svetlana Sagadeeva and Matthias Boehm. 2021. SliceLine: Fast, Linear-Algebra-based Slice Finding for ML Model Debugging. In *SIGMOD*. 2290–2299.
 - [36] Maximilian Schleich, Dan Olteanu, Mahmoud Abo Khamis, Hung Q. Ngo, and XuanLong Nguyen. 2019. A Layered Aggregate Engine for Analytics Workloads. In *SIGMOD*. 1642–1659.
 - [37] Maximilian Schleich, Dan Olteanu, and Radu Ciucanu. 2016. Learning Linear Regression Models over Factorized Joins. In *SIGMOD*. 3–18.
 - [38] Erhard Schmidt. 1907. Zur Theorie der linearen und nichtlinearen Integralgleichungen. *Math. Ann.* 63, 4 (1907), 433–476.
 - [39] Alok Sharma, Kuldip K. Paliwal, Seiya Imoto, and Satoru Miyano. 2013. Principal component analysis using QR decomposition. *Int. J. Mach. Learn. Cybern.* 4, 6 (2013), 679–683.
 - [40] Johanna Sommer, Matthias Boehm, Alexandre V. Evfimievski, Berthold Reinwald, and Peter J. Haas. 2019. MNC: Structure-Exploiting Sparsity Estimation for Matrix Expressions. In *SIGMOD*. 1607–1623.
 - [41] G. W. Stewart. 1998. *Matrix Algorithms*. Society for Industrial and Applied Mathematics.
 - [42] Panruo Wu and Zizhong Chen. 2014. FT-ScaLAPACK: correcting soft errors on-line for ScaLAPACK cholesky, QR, and LU factorization routines. In *High-Performance Parallel and Distributed Computing*. 49–60.
 - [43] Weipeng P. Yan and Per-Åke Larson. 1995. Eager Aggregation and Lazy Aggregation. In *VLDB*. 345–357.
 - [44] Yelp. 2017. Yelp Dataset Challenge. <https://www.yelp.com/dataset/challenge/>
 - [45] Binhang Yuan, Dimitrije Jankov, Jia Zou, Yuxin Tang, Daniel Bourgeois, and Chris Jermaine. 2021. Tensor Relational Algebra for Distributed Machine Learning System Design. *Proc. VLDB Endow.* 14, 8 (2021), 1338–1350.
 - [46] Reza Bosagh Zadeh, Xiangrui Meng, Alexander Ulanov, Burak Yavuz, Li Pu, Shivaram Venkataraman, Evan R. Sparks, Aaron Staple, and Matei Zaharia. 2016. Matrix Computations and Optimization in Apache Spark. In *SIGKDD*. 31–38.